Knizhnik-Zamolodchikov equations and integrable Landau-Zener models

Suvendu Barik[1⋆], Lieuwe Bakker[1†], Vladimir Gritsev[1, 2‡] and Emil Yuzbashyan[3§]

1 Institute for Theoretical Physics, Universiteit van Amsterdam, Science Park 904, 1098XH Amsterdam, The Netherlands
2 Russian Quantum Center, Skolkovo, Moscow 143025, Russia
3 Department of Physics and Astronomy, Center for Materials Theory, Rutgers University, Piscataway, New Jersey 08854 USA

⋆ s.k.barik@uva.nl , † l.bakker@friam.nl, ‡ v.gritsev@uva.nl, § eyuzbash@physics.rutgers.edu

Abstract

We study the relationship between integrable Landau-Zener (LZ) models and Knizhnik-Zamolodchikov (KZ) equations. The latter are originally equations for the correlation functions of two-dimensional conformal field theories, but can also be interpreted as multi-time Schrödinger equations. The general LZ problem is to find the probabilities of tunneling from eigenstates at $t = t_{\text{in}}$ to the eigenstates at $t \to +\infty$ for an $N \times N$ time-dependent Hamiltonian $\hat{H}(t)$. A number of such problems are exactly solvable in the sense that the tunneling probabilities are elementary functions of Hamiltonian parameters and time-dependent wavefunctions are special functions. It has recently been proposed that exactly solvable LZ models map to KZ equations. Here we use this connection to identify and solve various integrable hyperbolic LZ models $\hat{H}(t) = \hat{A} + \hat{B}/t$ for $N = 2, 3,$ and 4, where $\hat{A}$ and $\hat{B}$ are time-independent matrices. Some of these models have been considered, though not fully solved, before and others are entirely new.

Received Date
Accepted Date
Published Date

Contents

1 Introduction

Exploring the dynamics of avoided crossings in energy levels is a well known venture in physics. Famously, they were studied in the context of one-dimensional, slow atomic collisions by Landau [1] and intra-molecular level transitions by Zener [2] in 1932. In the same year, Majorana [3] extensively studied a spin-$1/2$ system in a varying magnetic field while Stückelberg [4] utilized JWKB theory to solve the corresponding differential equations. All of them essentially set out to determine the probability of an initial state transitioning to another eigenstate of the Hamiltonian as a function of time. This probability is referred to as the 'transition probability' and was initially studied in the non-adiabatic evolution of two-level systems. The results obtained have proven to be of integral importance to many advancements. For instance, Majorana's work explained the 'holes' in the magneto-optical traps used in the first realisation of a BEC[1] [5].

The Landau-Zener-Stückelberg-Majorana problem (LZSM or LZ in short)[2] [6] is well known in the studies of ions and molecules placed within a time-varying field. To calculate the transition probabilities of multi-state systems (i.e. systems of dimension $N \times N$, $N > 2$), it may suffice to look at the avoided crossings of two instantaneous energy levels. Hence, transition probabilities of these multi-state systems simplify into a product of transition probabilities at each crossing where the probabilities are given by a linearised 2×2 LZ model as solved by Landau, Zener and the others. A schematic description of the setting is given in Fig 1.

[1]The question on how to avoid these 'Majorana holes' was resolved by Ketterle by simply 'plugging' the hole using a focused laser.

[2]In this work we will refer to this problem as the 'LZ problem' for brevity.

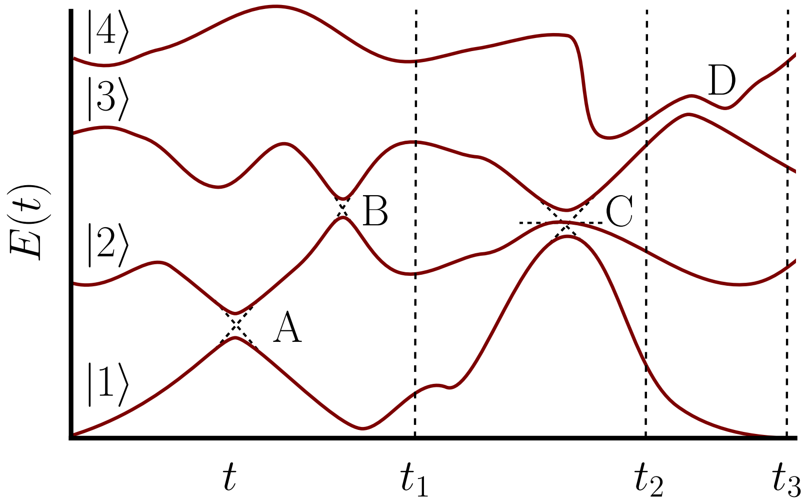

Figure 1: Schematic depiction of adiabatic (instantaneous) energy levels labeled by $|\alpha\rangle$ for $\alpha = \{1\ldots,4\}$. As an example, consider the transition probability $P_{|1\rangle\to|3\rangle}$ starting from $t = 0$. At t_1 it can be computed using standard 2×2 LZ problems defined at anticrossings A and B. The same probability at time t_2 requires a understanding of a higher order ($N = 3$) LZ problem at point C. Finding the probability at time t_3 requires the solution to a non-standard (i.e. nonlinear) LZ problem as depicted at point D.

Not surprisingly this simplification down to two level systems does not resolve the general setting of the problem. For example, when linear time dependence of the model is not sufficient (i.e. the level crossings cannot be linearised) or when the anti-crossing involves more than two energy levels, the transition probabilities cannot be readily calculated using the solutions found in 1932. Hence other varieties of the LZ problem require consideration. In the 90 years after the original papers of 1932, an assortment of these problems have been addressed.

Known exactly solvable LZ models with linear time dependence include the Demkov-Osherov model [7] where only a single diagonal matrix element is time dependent, the 'bow-tie' and 'generalized bow-tie' models [8–10] where all or most diabatic energy levels cross at a single point, and the many-body inhomogeneous Dicke model [11–13], which describes a bunch of two-level systems interacting with a single linear time-dependent bosonic mode (detuning). These models are exactly solvable in the sense that transition probabilities from $t = -\infty$ to $t = +\infty$ are found explicitly in terms of elementary functions.

A natural question to consider is; what is special about these and other similar LZ models that makes them exactly solvable? This question was addressed in [14] with the conclusion that the necessary condition for LZ solvability is the *quantum integrability* of the model, in the sense that there exist nontrivial, mutually commuting partners,

$$[\hat{H}_i(t), \hat{H}_j(t)] = 0, \quad i, j = 1, \ldots, n, \tag{1}$$

where $H_1(t) \equiv H(t)$ is the model (LZ) Hamiltonian and $H_i(t)$ with $i > 1$ are its commuting partners. With appropriate restrictions on $H_i(t)$ to make the condition (1) nontrivial, this is a good analog [15] of classical *Liouville integrability* [16]. In the aformentioned examples above, the $H_i(t)$ are required to be linear in t. For a nonlinear LZ model this requirement has to be generalized.

This quantum version of Liouville integrability is clearly only necessary and not sufficient for a LZ problem to be exactly solvable. Indeed, most quantum integrable models (e.g., the 1D Hubbard or XXZ Hamiltonians) do not turn into exactly solvable LZ models when we make their parameters (e.g., Hubbard U or the anisotropy in the XXZ Hamiltonian) depend on time in an arbitrary way. It has been conjectured in [12] that the necessary and sufficient condition is in fact the existence of a multi-time Schrödinger system of equations

$$i\nu\frac{\partial\Psi(\vec{z})}{\partial z_i}=\hat{H}_i\Psi(\vec{z}),\qquad i=1,\ldots,n. \tag{2}$$

Here $\vec{z}=(z_1,\ldots z_n)$ and ν are the parameters of the LZ model, one of which is the rescaled time variable, $z_1\equiv\nu t$. In other words, the first equation in (2) is the nonstationary Schrödinger equation of the original LZ problem, which we are seeking to solve. The remaining z_i, which play the role of additional 'times' in equation (2), are other parameters of the underlying LZ Hamiltonian. For example, in the inhomogeneous Dicke model z_i are the level splittings of the two-level systems while the energy of the bosonic mode ω changes at the rate ν, i.e., $\omega=-\nu t$.

The system of multi-time Schrödinger equations (2) is compatible if and only if the *Frobenius integrability* condition is satisfied,

$$\frac{\partial\hat{H}_i}{\partial z_j}-\frac{\partial\hat{H}_j}{\partial z_i}-i[\hat{H}_i,\hat{H}_j]=0,\quad i,j=1,\ldots,n. \tag{3}$$

To put it another way, the exact solvability of a LZ problem is equivalent to Frobenius rather than Liouville integrability [17]. Note that for real Hamiltonians ($\hat{H}_i^*=\hat{H}_i$) the real and imaginary parts of equation (3) separate into two conditions, one of which is equation (1) while the other reads

$$\frac{\partial\hat{H}_i}{\partial z_j}=\frac{\partial\hat{H}_j}{\partial z_i}. \tag{4}$$

Thus, in this context the Frobenius integrability is more restrictive than the Liouville one.

Essentially the only nontrivial example of a multi-time system (2) we are aware of, such that $\hat{H}_i$ admit a representation in terms of finite size matrices are the Knizhnik-Zamolodchikov (KZ) equations and their various generalizations. The original KZ equations [18] are differential equations for n-point correlation functions $\Psi(\vec{z})$ in Wess-Zumino-Witten models. In this case, $\hat{H}_i$ in equation (2) have the following form:

$$\hat{H}_i=\sum_{j\neq i,\alpha,\beta}\frac{\eta_{\alpha\beta}\hat{r}_i^\alpha\otimes\hat{r}_j^\beta}{z_j-z_i}, \tag{5}$$

where $\hat{r}_i^\alpha$ are the generators of a Lie algebra and η is its Killing form. These $\hat{H}_i$ are known as rational Gaudin magnets [19]. In addition, there are integrable hyperbolic, trigonometric, and elliptic Gaudin magnets [19, 20], where the 'couplings' $\frac{1}{z_i-z_j}$ are replaced by hyperbolic, trigonometric and elliptic functions of (z_i-z_j) that are also different for different values of α and β (anisotropic). Various boundary terms (terms that single out $\hat{r}_i^\alpha$) can be added to $\hat{H}_i$ without spoiling the integrability [20–25]. All these generalized Gaudin magnets satisfy the Frobenius integrability condition (3) and, therefore, give rise to integrable generalizations of KZ equations and, according to the above conjecture [12], to integrable LZ models.

Let us note here that, strictly speaking, we say that a LZ model is *integrable* when the Frobenius integrability condition (3) is satisfied and we say that it is *exactly solvable* when its transition amplitudes can be determined in terms of elementary functions and the time-dependent wavefunction in terms of known special functions.

This connection to the KZ equations does not solve all integrable LZ problems for us immediately. Unfortunately, the solution to the KZ equations is extremely complicated. It is written in terms of a multidimensional contour integral over the so-called Yang-Yang action, derived from the off-shell Bethe ansatz equations [26–29]. For a summary of results on the KZ equations, we refer to the Askey-Bateman Project: Volume 2 and references therein [30] as well as Aomoto's book on the cohomology methods in resolving such integrals [31]. As a result, applying the general solution of the KZ equations in practice remains a complicated endeavor. That is not to say that this solution is not already useful. For example, Zabalo et al. [32] used the general solution to provide an asymptotic solution to the hyperbolic time dependent spin-1/2 BCS Hamiltonian for any system size at large time through a saddle point approximation.

The purpose of the present paper is to initiate a systematic construction and explicit solution to the integrable LZ models of physical interest by utilizing their link to the KZ equations. Specifically, we derive here several simplest nontrivial examples of integrable LZ models from the KZ equations, solve them directly, and extract their solution from the contour integral solution of the KZ equations.

We focus on the case when it is impossible to describe LZ tunneling by linearizing the anticrossings. In particular, when one considers collisions of, for example, atoms and ions, the electromagnetic potentials involved are inversely proportional to the radius. In this scenario, assuming a constant velocity, the LZ Hamiltonian is of the form $\hat{H}(t) = \hat{A} + \hat{B}/t$, where $\hat{A}$ and $\hat{B}$ are time-independent Hermitian operators. These type of problems were originally dubbed as 'Coulomb' LZ problems, referring to the Coulomb potential involved [33–37]. Alternatively, these Coulomb models can be described by Nikitin's [38] exponential models through a simple transformation described in Section 2. We note that we prefer calling such LZ problems Hyperbolic LZ (HLZ) problems, to accommodate more general physical setups. There are plethora of reasons to study hyperbolic LZ models. Table III in [38] gives some nice examples such as the ion-atom collisions stated above and transitions between vibrational modes [39]. These problems also manifest in Rydberg transitions and molecular collisions. See for examples Refs. [25-26] in [40] and Ref. [41].

This work is structured as follows. In Section 2 we start with basic 2×2 and 3×3 HLZ Hamiltonians, some of which were previously considered in [40]. Full analytical solutions of the non-stationary Schrödinger equation for these models are presented and the resulting transition probabilities are obtained. The second part of this work in Section 3 shows how these models arise from the general prescription of the KZ equations. We demonstrate the relationship between the HLZ problems and the BCS (a.k.a. Richardson or Richardson-Gaudin) model with the superconducting coupling inversely proportional to time as discussed in [13] and [32]. Then, we show how our initially introduced HLZ models are solved by means of contour integration, elucidating our understanding of the 'contour conundrum' posed by the formal solution of the KZ equations. Finally, in Section 2 we identify a number of new integrable multi-level HLZ models through the KZ connection. We do not seek to fully solve all of these new models, but do derive several explicit exact solutions of their non-stationary Schrödinger equations as an example. We conclude by discussing our results and outlining outstanding problems and topics of further interest in the Conclusion & Discussion.

2 Hyperbolic Landau-Zener models

The general form of the hyperbolic Landau-Zener (HLZ) model is

$$i\partial_t \Psi(t) = \left(\hat{A} + \frac{1}{t}\hat{B}\right)\Psi(t) \tag{6}$$

where $\hat{A}$ and $\hat{B}$ are constant, Hermitian matrices written in the diabatic basis defined through diagonalising $\hat{B}$ by a orthogonal transformation. The evolution begins at $t \to 0^+$ and proceeds towards the positive direction of infinity.

We immediately note that the differential equations (6), when transformed by the substitution $t = e^{\lambda}$ is written as

$$i\partial_\lambda \Psi(\lambda) = \left[\hat{B} + e^{\lambda}\hat{A}\right]\Psi(\lambda), \tag{7}$$

where $\lambda \to -\infty$ is equivalent to $t \to 0^+$ and $\lambda \to \infty$ points to $t \to \infty$. This shows that one can transform any HLZ model to an exponential LZ problem through a simple substitution [35].

After rewriting (6) in the diabatic basis, we can reduce one of the diagonal terms to zero by removing an overall prefactor contributing a (time dependent) global phase to the wavefunction. Then, the lowest non-trivial representation (for real-symmetric matrices) of the problem is given by

$$i\begin{pmatrix}\dot{\psi}_1(t)\\ \dot{\psi}_2(t)\end{pmatrix} = \begin{pmatrix}\frac{p}{t}+a_1 & a_2\\ a_2 & 0\end{pmatrix}\begin{pmatrix}\psi_1(t)\\ \psi_2(t)\end{pmatrix}. \tag{8}$$

This problem is referred to in this manuscript as the '2×2 HLZ' problem. While it has been extensively studied in the literature since the 1970s [33–37,40], we provide a general solution in this work. In the main text, we focus on the case $a_1 = 0$ and set the remaining parameters as

$$\left\{p = -\frac{1}{\nu},\ a_1 = 0,\ a_2 = -\Delta\right\}, \tag{9}$$

while the case $a_1 \neq 0$ is addressed in the appendix A.2 for completeness. The 3×3 HLZ problem is generally not solvable in terms of known special functions. The same applies to the general 3×3 LZ problem linear in t. However, there turns out to be a particular version of the HLZ problem which is solvable,

$$i\begin{pmatrix}\dot{\psi}_1(t)\\ \dot{\psi}_2(t)\\ \dot{\psi}_3(t)\end{pmatrix} = \begin{pmatrix}\frac{p}{t} & a_1 & 0\\ a_1 & \frac{q}{t} & a_2\\ 0 & a_2 & 0\end{pmatrix}\begin{pmatrix}\psi_1(t)\\ \psi_2(t)\\ \psi_3(t)\end{pmatrix}. \tag{10}$$

In this section, we solve this problem for

$$\left\{p = -\frac{3}{\nu},\ q = -\frac{1}{\nu},\ a_1 = -\frac{2\Delta}{\sqrt{3}},\ a_2 = 2\sqrt{\frac{2}{3}}\Delta\right\}, \tag{11}$$

where Δ and ν are real-valued constants. While the model for the parameters above has been addressed previously [40], the general solution of (10) provided in this work is new.

The goal of the LZ problem is to calculate the aptly named transition probability matrix. For a $N \times N$ problem, this matrix is written as

$$P_{N\times N} = \begin{pmatrix} p_{1\to 1} & p_{1\to 2} & \cdots & p_{1\to N}\\ p_{2\to 1} & p_{2\to 2} & \cdots & p_{2\to N}\\ \vdots & \vdots & \ddots & \vdots\\ p_{N\to 1} & p_{N\to 2} & \cdots & p_{N\to N}\end{pmatrix}. \tag{12}$$

Here, 1 refers to the ground state, 2 to the first excited state and so forth, up to N being the highest excited state. $p_{m\to n}$ is the probability for the system starting in the $(m)^{\text{th}}$ state at the initial time to end up in the $(n)^{\text{th}}$ state at the final time. As mentioned earlier, for the HLZ problems presented here, the initial and final times are $t = 0^+$ and $t \to \infty$, respectively.

2.1 Evolution from the ground state

Let us write $|\psi(t)\rangle = \psi_1(t)|1\rangle + \psi_2(t)|2\rangle$, where the ground state is $|1\rangle$ and the next excited state is $|2\rangle$ and so on, all of which are in the canonical basis. The solution of the nonstationary Schrödinger equation (8) with parameters (9) is (with $\tau = t\Delta$)

$$|\psi^1_{1/2,0}(\tau)\rangle = \left(\frac{\pi}{2\cosh\frac{\pi}{2\nu}}\right)^{1/2} \tau^{\frac{1}{2}+\frac{i}{2\nu}} \left[J_{\frac{1}{2}+\frac{i}{2\nu}}(\tau)|2\rangle - iJ_{-\frac{1}{2}+\frac{i}{2\nu}}(\tau)|1\rangle\right], \tag{13}$$

where $J_\alpha(t)$ is the Bessel function of the first kind. The superscript 1 indicates that the boundary condition at $t = 0$ is the ground state. The subscripts $1/2$ and 0 describe the state in the corresponding BCS problem, which which will be further explained in Section 3. The solution of the 3×3 problem defined by (10) and (11) is (using the same notation and boundary condition as above)

$$|\psi^1_{1,0}(\tau)\rangle = \phi^1_1(\tau)|1\rangle + \phi^1_2(\tau)|2\rangle + \phi^1_3(\tau)|3\rangle\,, \tag{14}$$

with

$$\phi^1_1(\tau) = e^{\frac{3i}{\nu}\ln(\tau)}\, {}_1F_2\left[{\frac{i}{2\nu} \atop \frac{1}{2}+\frac{i}{\nu},\frac{3i}{2\nu}};-\tau^2\right], \tag{15a}$$

$$\phi^1_2(\tau) = \frac{2i\nu\tau e^{\frac{3i}{\nu}\ln(\tau)}}{(2i+\nu)\sqrt{3}}\, {}_1F_2\left[{1+\frac{i}{2\nu} \atop \frac{3}{2}+\frac{i}{\nu},1+\frac{3i}{2\nu}};-\tau^2\right], \tag{15b}$$

$$\phi^1_3(\tau) = \frac{e^{\frac{3i}{\nu}\ln(\tau)}}{\sqrt{2}}\left({}_1F_2\left[{\frac{i}{2\nu} \atop \frac{1}{2}+\frac{i}{\nu},\frac{3i}{2\nu}};-\tau^2\right] - {}_1F_2\left[{1+\frac{i}{2\nu} \atop \frac{3}{2}+\frac{i}{\nu},1+\frac{3i}{2\nu}};-\tau^2\right]\right) \tag{15c}$$
$$+ \frac{2\sqrt{2}\nu^2(2\nu+i)\tau^2 e^{\frac{3i}{\nu}\ln(\tau)}}{(2\nu+3i)(\nu+2i)(3\nu+2i)}\, {}_1F_2\left[{2+\frac{i}{2\nu} \atop \frac{5}{2}+\frac{i}{\nu},2+\frac{3i}{2\nu}};-\tau^2\right].$$

Here, the function ${}_pF_q\left[{a \atop b\ c};t\right]$ is a generalized hypergeometric function.[3]

2.2 Evolution from excited states

The solutions to the differential equations (8) and (10) can be determined for any general choice of initial conditions. In order to obtain all transition probabilities, the problem must also be solved for the initial conditions being the excited state(s). For the 2×2 problem, the only excited state at the initial time $t \to 0^+$ is $|2\rangle$. The wavefunction starting from $|2\rangle$ is given by

$$|\psi^2_{1/2,0}(\tau)\rangle = \left(\frac{\pi}{2\cosh\frac{\pi}{2\nu}}\right)^{1/2} \tau^{\frac{1}{2}+\frac{i}{2\nu}} \left[J_{-\frac{1}{2}-\frac{i}{2\nu}}(\tau)|2\rangle + iJ_{\frac{1}{2}-\frac{i}{2\nu}}(\tau)|1\rangle\right]. \tag{16}$$

For the 3×3 problem, we have the excited states $|2\rangle$ and $|3\rangle$, where $|3\rangle$ is the highest energy level. The solutions to the Schrödinger equations starting from the excited states are then given as follows:

$$|\psi^k_{1,0}(\tau)\rangle = \mathcal{N}_k\left[\phi^k_1(\tau)|1\rangle + \phi^k_2(\tau)|2\rangle + \phi^k_3(\tau)|3\rangle\right], \quad k = 2,3, \tag{17}$$

[3] Not to be confused with the 'general hypergeometric functions' or 'Gelfand-Aomoto hypergeometric functions' which are also ubiquitous in literature regarding KZ equations [30].

with

$$\phi_1^2(\tau) = \tau e^{\frac{i}{\nu}\ln(\tau)}\,{}_1F_2\left[\begin{matrix}\frac{1}{2}-\frac{i}{2\nu}\\ \frac{1}{2}+\frac{i}{2\nu},\frac{3}{2}-\frac{i}{\nu}\end{matrix};-\tau^2\right], \tag{18a}$$

$$\phi_1^3(\tau) = \tau^2\,{}_1F_2\left[\begin{matrix}1-\frac{i}{\nu}\\ \frac{3}{2}-\frac{i}{2\nu},2-\frac{3i}{2\nu}\end{matrix};-\tau^2\right], \tag{18b}$$

$$\phi_2^2(\tau) = i\sqrt{3}e^{\frac{i}{\nu}\ln(\tau)}\left[\frac{(-\nu+2i)}{2\nu}\,{}_1F_2\left[\begin{matrix}\frac{1}{2}-\frac{i}{2\nu}\\ \frac{1}{2}+\frac{i}{2\nu},\frac{3}{2}-\frac{i}{\nu}\end{matrix};-\tau^2\right]\right. \\ \left.+\frac{2\nu(\nu-i)\tau^2}{(\nu+i)(3\nu-2i)}\,{}_1F_2\left[\begin{matrix}\frac{3}{2}-\frac{i}{2\nu}\\ \frac{3}{2}+\frac{i}{2\nu},\frac{5}{2}-\frac{i}{\nu}\end{matrix};-\tau^2\right]\right], \tag{18c}$$

$$\phi_2^3(\tau) = i\sqrt{3}\tau\left[\frac{(-2\nu+3i)}{2\nu}\,{}_1F_2\left[\begin{matrix}1-\frac{i}{\nu}\\ \frac{3}{2}-\frac{i}{2\nu},2-\frac{3i}{2\nu}\end{matrix};-\tau^2\right]\right. \\ \left.+\frac{4\nu(\nu-i)\tau^2}{(3\nu-i)(4\nu-3i)}\,{}_1F_2\left[\begin{matrix}2-\frac{i}{\nu}\\ \frac{5}{2}-\frac{i}{2\nu},3-\frac{3i}{2\nu}\end{matrix};-\tau^2\right]\right], \tag{18d}$$

$$\phi_3^2(\tau) = \frac{\tau e^{\frac{i}{\nu}\ln(\tau)}}{\sqrt{2}}\left[{}_1F_2\left[\begin{matrix}\frac{1}{2}-\frac{i}{2\nu}\\ \frac{1}{2}+\frac{i}{2\nu},\frac{3}{2}-\frac{i}{\nu}\end{matrix};-\tau^2\right]-\frac{3(\nu-i)}{(\nu+i)}\,{}_1F_2\left[\begin{matrix}\frac{3}{2}-\frac{i}{2\nu}\\ \frac{3}{2}+\frac{i}{2\nu},\frac{5}{2}-\frac{i}{\nu}\end{matrix};-\tau^2\right]\right] \\ +\frac{6\sqrt{2}\nu^2(\nu-i)(3\nu-i)\tau^3 e^{\frac{i}{\nu}\ln(\tau)}}{(\nu+i)(3\nu+i)(3\nu-2i)(5\nu-2i)}\,{}_1F_2\left[\begin{matrix}\frac{5}{2}-\frac{i}{2\nu}\\ \frac{5}{2}+\frac{i}{2\nu},\frac{7}{2}-\frac{i}{\nu}\end{matrix};-\tau^2\right], \tag{18e}$$

$$\phi_3^3(\tau) = \left[\frac{3(\nu-i)(2\nu-3i)}{4\sqrt{2}\nu^2}+\frac{\tau^2}{\sqrt{2}}\right]{}_1F_2\left[\begin{matrix}1-\frac{i}{\nu}\\ \frac{3}{2}-\frac{i}{2\nu},2-\frac{3i}{2\nu}\end{matrix};-\tau^2\right]-\frac{3\sqrt{2}(\nu-i)(5\nu-4i)\tau^2}{(3\nu-i)(4\nu-3i)}\times \\ {}_1F_2\left[\begin{matrix}2-\frac{i}{\nu}\\ \frac{5}{2}-\frac{i}{2\nu},3-\frac{3i}{2\nu}\end{matrix};-\tau^2\right]+\frac{8\sqrt{2}\nu^2(\nu-i)\tau^4}{(3\nu-i)(4\nu-3i)(5\nu-i)}\,{}_1F_2\left[\begin{matrix}3-\frac{i}{\nu}\\ \frac{7}{2}-\frac{i}{2\nu},4-\frac{3i}{2\nu}\end{matrix};-\tau^2\right], \tag{18f}$$

and

$$\mathcal{N}_2 = \left(\frac{3}{4}+\frac{3}{\nu^2}\right)^{-1/2} \quad \text{and} \quad \mathcal{N}_3 = \left[\frac{9\left(\nu^2+1\right)\left(4\nu^2+9\right)}{32\nu^4}\right]^{-1/2}. \tag{18g}$$

This concludes the complete system of solutions to the problems described in this section. Below, we introduce several notations for the basis states that will prove useful in the upcoming section. Firstly,

$$|1/2,0\rangle_g \equiv \frac{1}{\sqrt{2}}(|\uparrow\downarrow\rangle+|\downarrow\uparrow\rangle) \quad \text{and} \quad |1,0\rangle_g \equiv \frac{1}{\sqrt{6}}(|1,\text{-}1\rangle+2\,|0,0\rangle+|\text{-}1,1\rangle). \tag{19}$$

Here, as with the notation for the wavefunctions before, the quantum numbers on the LHS characterize the state as in the BCS Hamiltonian from which this problem is derived. For the 2×2 model we use

$$|1\rangle = |1/2,0\rangle_g\,,\ |2\rangle = \frac{1}{\sqrt{2}}(|\uparrow\downarrow\rangle-|\downarrow\uparrow\rangle). \tag{20a}$$

Finally for the 3×3 model we use

$$|1\rangle = |1,0\rangle_g\,,\quad |2\rangle = \frac{1}{\sqrt{2}}(|1,\text{-}1\rangle-|\text{-}1,1\rangle),\quad |3\rangle = \frac{1}{\sqrt{3}}(-|\text{-}1,1\rangle+|0,0\rangle-|1,\text{-}1\rangle). \tag{20b}$$

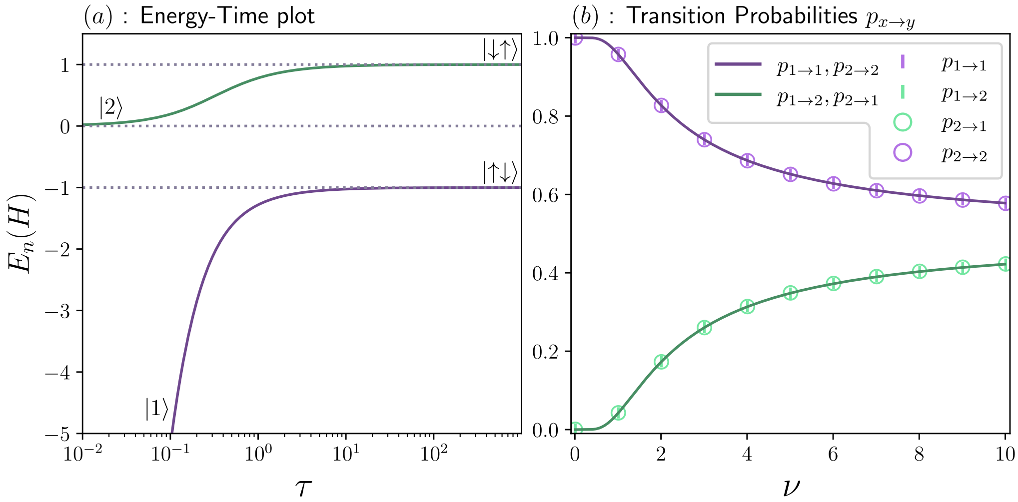

Figure 2: (a) Instantaneous (adiabatic) eigenvalues of the 2×2 HLZ model as functions of $\tau = t\Delta$ for $\nu = 2$. The ground state $|1\rangle$ evolves towards $|\uparrow\downarrow\rangle$ (purple curve). The excited state $|2\rangle$ ends up in $|\downarrow\uparrow\rangle$ (green curve). (b) Elements of the transition probability matrices. Solid lines represent the analytical expressions in (22). The scatter plots represent the numerical simulation of $p_{x\to y}$ at $\tau = 10^3$.

2.3 Transition probabilities

2.3.1 The 2×2 HLZ problem

At $t = 0^+$, the ground state of the 2×2 HLZ model is $|1/2,0\rangle_g$ in (19). At $t\to\infty$, it becomes $|\uparrow\downarrow\rangle$. The large-time asymptotes of the solutions (13) and (16) read

$$|\psi^1_{1/2,0}(\tau)\rangle \to -i\left(\frac{1}{2\cosh\frac{\pi}{2\nu}}\right)^{1/2}\exp\left(\frac{i\ln\tau}{2\nu}\right)\left(e^{i\tau}e^{\frac{\pi}{4\nu}}|\uparrow\downarrow\rangle + e^{-i\tau}e^{-\frac{\pi}{4\nu}}|\downarrow\uparrow\rangle\right), \tag{21a}$$

$$|\psi^2_{1/2,0}(\tau)\rangle \to -\left(\frac{1}{2\cosh\frac{\pi}{2\nu}}\right)^{1/2}\exp\left(\frac{i\ln\tau}{2\nu}\right)\left(e^{i\tau}e^{-\frac{\pi}{4\nu}}|\uparrow\downarrow\rangle - e^{-i\tau}e^{\frac{\pi}{4\nu}}|\downarrow\uparrow\rangle\right). \tag{21b}$$

This implies

$$P_{2\times2} = \frac{1}{e^{\frac{\pi}{2\nu}} + e^{-\frac{\pi}{2\nu}}}\begin{pmatrix} e^{\frac{\pi}{2\nu}} & e^{-\frac{\pi}{2\nu}} \\ e^{-\frac{\pi}{2\nu}} & e^{\frac{\pi}{2\nu}} \end{pmatrix}. \tag{22}$$

Fig. 2 shows these transition probabilities, alongside the spectrum of the 2×2 model for various choices of ν at large $\tau = \Delta t$.

2.3.2 The 3×3 HLZ problem

The ground state of the 3×3 HLZ model at $t = 0^+$ is $|1,0\rangle_g$ in (19). At $t\to\infty$, it becomes $|1,-1\rangle$. Evaluating the asymptotic behaviour of the solutions (14) and (17) at large time, we

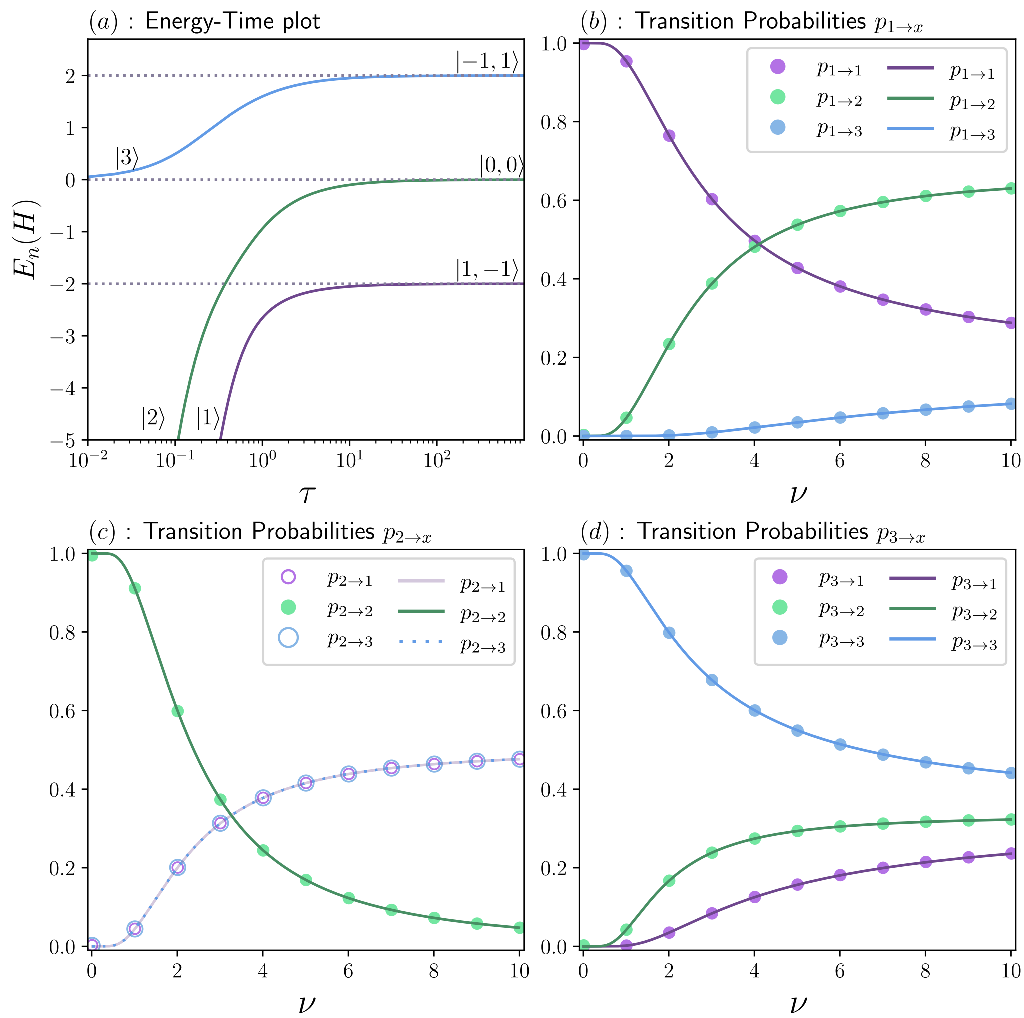

Figure 3: (a) Instantaneous eigenvalues vs $\tau = t\Delta$ for the 3×3 HLZ model with parameters (11) ($\nu = 2$). The ground state $|1\rangle$ evolves towards $|1,-1\rangle$ (purple curve). $|2\rangle$ and $|3\rangle$ evolve to $|0,0\rangle$ (green curve) and $|-1,1\rangle$ (blue curve), respectively. (b–d) Transition probabilities. The solid lines represent the analytical expressions in (24). The scatter plots are the numerical simulation of $p_{x\to y}$ for different values of ν evaluated at $\tau = 10^3$.

find

$$|\psi^1_{1,0}(\tau)\rangle \to C_1 \tau^{\frac{2i}{\nu}} \left[e^{\frac{\pi}{\nu}+2i\tau-\frac{i}{\nu}\ln\tau} |1,\text{-}1\rangle + \frac{2\pi e^{-\frac{i}{\nu}\ln 2}}{\Gamma\left(\frac{i}{2\nu}+\frac{1}{2}\right)^2} |0,0\rangle + e^{-\left(\frac{\pi}{\nu}+2i\tau+\frac{i}{\nu}\ln\tau\right)} |\text{-}1,1\rangle \right], \quad (23a)$$

$$|\psi^2_{1,0}(\tau)\rangle \to C_2 \tau^{\frac{2i}{\nu}} \sinh\left(\frac{\pi}{2\nu}\right) \left[e^{-\frac{i}{\nu}\ln\tau} \left(|1,\text{-}1\rangle - |\text{-}1,1\rangle\right) + \frac{i\sqrt{\pi}\,\Gamma\left(\frac{1}{2}-\frac{i}{2\nu}\right)}{\Gamma\left(1-\frac{i}{2\nu}\right)\Gamma\left(\frac{i}{\nu}\right)} |0,0\rangle \right], \quad (23b)$$

$$|\psi^3_{1,0}(\tau)\rangle \to C_3 \tau^{\frac{2i}{\nu}} \left[\frac{e^{2i\tau-\frac{i}{\nu}\ln\tau}}{1+e^{\frac{\pi}{\nu}}} |1,\text{-}1\rangle - \frac{e^{-\frac{i}{\nu}\ln 2}\,\Gamma\left(\frac{-i+\nu}{2\nu}\right)}{2\Gamma\left(\frac{i+\nu}{2\nu}\right)\cosh\left(\frac{\pi}{2\nu}\right)} |0,0\rangle + \frac{e^{\frac{\pi}{\nu}-2i\tau-\frac{i}{\nu}\ln\tau}}{1+e^{\frac{\pi}{\nu}}} |\text{-}1,1\rangle \right]. \quad (23c)$$

Here,

$$C_1 = \frac{\sqrt{\frac{3}{2\pi}}\Gamma\left(\frac{1}{2}+\frac{i}{\nu}\right)\Gamma\left(\frac{3i}{2\nu}\right)}{\Gamma\left(\frac{i}{2\nu}\right)}, \quad C_2 = \mathcal{N}_2\sqrt{\frac{3}{2}}e^{\frac{2i}{\nu}\ln 2}\frac{\Gamma\left(2-\frac{2i}{\nu}\right)\Gamma\left(\frac{i}{\nu}\right)}{\Gamma\left(\frac{1}{2}-\frac{i}{2\nu}\right)^2}, \tag{23d}$$

and

$$C_3 = \mathcal{N}_3\frac{\sqrt{6\pi}\Gamma\left(2-\frac{3i}{2\nu}\right)}{\Gamma\left(-\frac{1}{2}+\frac{i}{2\nu}\right)\Gamma\left(1-\frac{i}{\nu}\right)}. \tag{23e}$$

The transition probability matrix is

$$P_{3\times 3} = \begin{pmatrix} \frac{1}{\left(1+e^{-\frac{2\pi}{\nu}}\right)\left(1+e^{-\frac{\pi}{\nu}}+e^{-\frac{2\pi}{\nu}}\right)} & \frac{e^{-\frac{\pi}{\nu}}\left(1+e^{-\frac{\pi}{\nu}}\right)^2}{\left(1+e^{-\frac{2\pi}{\nu}}\right)\left(1+e^{-\frac{\pi}{\nu}}+e^{-\frac{2\pi}{\nu}}\right)} & \frac{e^{-\frac{4\pi}{\nu}}}{\left(1+e^{-\frac{2\pi}{\nu}}\right)\left(1+e^{-\frac{\pi}{\nu}}+e^{-\frac{2\pi}{\nu}}\right)} \\ \frac{1}{2\cosh\left(\frac{\pi}{\nu}\right)} & 1-\frac{1}{\cosh\left(\frac{\pi}{\nu}\right)} & \frac{1}{2\cosh\left(\frac{\pi}{\nu}\right)} \\ \frac{1}{1+e^{\frac{\pi}{\nu}}+e^{\frac{2\pi}{\nu}}} & \frac{1}{2\cosh\left(\frac{\pi}{\nu}\right)+1} & \frac{1}{1+e^{-\frac{\pi}{\nu}}+e^{-\frac{2\pi}{\nu}}} \end{pmatrix}. \tag{24}$$

A plot of the transition probabilities, alongside the adiabatic spectrum of the 3×3 HLZ model for various choices of ν at large $\tau = \Delta t$ is provided in Figure 3.

Thus, we conclude our brute force investigation of the two hyperbolic Landau-Zener problems. The transition probabilities derived in this section have also been found through other means by Sinitsyn [40], who used symmetries and the no-go constraints for solving the transition probability matrix. For these models, however, a full solution in terms of wavefunctions is now also available. We note that the method of constructing the probability matrix through the constraints and symmetries remain insufficient for larger integrable LZ models that we consider in subsequent sections.

3 Generalised KZ equations and the BCS Hamiltonian

For the second part of the paper, we investigate the relationship of HLZ models and a set of integrable, time-dependent Richardson-Gaudin hamiltonians. More specifically, we show that these models belong to a class of problems that are solved by the formal solution to the KZ equations. The solutions of the KZ equations is expressed in terms of contour integrals. In practice, however, it is unclear how these integrals should be evaluated. The solution to the HLZ models presented in section 2 provide a valuable stepping stone to making sense of the aforementioned contours and, by extension, a larger class of time-dependent, many-body quantum systems.

3.1 Preliminaries

The generalised Knizhnik-Zamolodchikov equations we will use in this paper are of the form [13, 22, 25]

$$\begin{aligned} i\nu\frac{\partial \Psi}{\partial \varepsilon_j} &= \hat{H}_j\Psi, \quad j = 1,\ldots,N, \\ i\nu\frac{\partial \Psi}{\partial \Omega} &= \hat{H}_\Omega\Psi, \end{aligned} \tag{25}$$

where

$$\hat{H}_j = 2\Omega \hat{s}^z_j - \sum_{k \neq j} \frac{\hat{\mathbf{s}}_j \cdot \hat{\mathbf{s}}_k}{\varepsilon_j - \varepsilon_k}, \quad \hat{H}_\Omega = 2\sum_{j=1}^{N} \varepsilon_j \hat{s}^z_j - \frac{1}{2\Omega} \sum_{j,k} s^+_j s^-_k. \tag{26}$$

Let $\Omega \equiv \Omega(t)$ be a function of time. Then, the second equation in (25) becomes the non-stationary Schrödinger equation for the time-dependent BCS (a.k.a. Richardson) Hamiltonian

$$\hat{H}_{\text{BCS}}(t) \equiv \hat{H}_\Omega(t) = 2\nu^{-1}\dot{\Omega} \sum_j \varepsilon_j \hat{s}^z_j - (2\nu\Omega)^{-1}\dot{\Omega} \sum_{j,k} \hat{s}^+_j \hat{s}^-_k. \tag{27}$$

In this work $\Omega(t) = \nu t$, which yields a BCS Hamiltonian with the coupling inversely proportional to time:

$$\hat{H}_{\text{BCS}}(t) = 2\sum_j \varepsilon_j \hat{s}^z_j - \frac{1}{2\nu t} \sum_{j,k} \hat{s}^+_j \hat{s}^-_k. \tag{28}$$

Note that $\hat{s}_j$ are general spin operators of arbitrary magnitude s. The parameters ϵ_j play the role of on-site Zeeman magnetic fields. In the original fermion language, ϵ_j are the single-particle energy levels [42–44].

3.1.1 Two-site BCS models

In the basis where the z-component of the total spin is diagonal, the Hamiltonian (28) is block diagonal, with each block corresponding to a particular value of $S^z \in \{-sN, \ldots, sN\}$, i.e., $H_{\text{BCS}} = \bigoplus_{S^z=-sN}^{sN} H^{(S^z)}_{\text{BCS}}$. We note that, starting from this section, a spin-label is added to any operators to make the representations explicit. This is the same spin label as originally introduced in equations (13)-(17).

Beginning with spin-$1/2$, we have

$$\hat{s}^z_{1/2} = \frac{1}{2}\begin{pmatrix} 1 & 0 \\ 0 & -1 \end{pmatrix}, \quad \hat{s}^+_{1/2} = \begin{pmatrix} 0 & 1 \\ 0 & 0 \end{pmatrix}, \quad \hat{s}^-_{1/2} = \begin{pmatrix} 0 & 0 \\ 1 & 0 \end{pmatrix}. \tag{29}$$

We can write $\Psi(t)$ for $N = 2$ as

$$\Psi(t) = \sum_{i,j \in \{\uparrow,\downarrow\}} \psi_{i,j}(t) \, |i\rangle \otimes |j\rangle, \tag{30}$$

where $|i\rangle$ is the eigenstate of $\hat{s}^z_{1/2}$ in (29). By rewriting the eigenstate into a column vector with elements $\psi_{i,j}(t)$ with ordering of the (i,j) indices as $[(\downarrow,\downarrow),(\uparrow,\downarrow),(\downarrow,\uparrow),(\uparrow,\uparrow)]$, we have

$$\hat{H}_{\text{BCS},1/2} = \begin{pmatrix} H^{(-1)}_{1/2} & \cdot & \cdot \\ \cdot & H^{(0)}_{1/2} & \cdot \\ \cdot & \cdot & H^{(1)}_{1/2} \end{pmatrix}, \tag{31}$$

where

$$H^{(-1)}_{1/2}(\nu) = -(\varepsilon_1 + \varepsilon_2), \tag{32a}$$

$$H^{(1)}_{1/2}(\nu) = (\varepsilon_1 + \varepsilon_2) - \frac{1}{\nu t}, \tag{32b}$$

$$H^{(0)}_{1/2}(\nu) = (\varepsilon_1 - \varepsilon_2)\sigma^z - \frac{1}{2\nu t}(\mathbb{I} + \sigma^x), \tag{32c}$$

and σ^i are the usual Pauli matrices. After the unitary transformation defined by Eqs. (19) and (20a) and for $\Delta = \varepsilon_2 - \varepsilon_1$ with $\varepsilon_2 > \varepsilon_1$, the $S^z = 0$ sector is identified as the 2×2 HLZ problem in equation (8).

Consider now spin-1,

$$\hat{s}_1^z = \begin{pmatrix} 1 & 0 & 0 \\ 0 & 0 & 0 \\ 0 & 0 & -1 \end{pmatrix}, \quad \hat{s}_1^+ = \sqrt{2}\begin{pmatrix} 0 & 1 & 0 \\ 0 & 0 & 1 \\ 0 & 0 & 0 \end{pmatrix}, \quad \hat{s}_1^- = \sqrt{2}\begin{pmatrix} 0 & 0 & 0 \\ 1 & 0 & 0 \\ 0 & 1 & 0 \end{pmatrix}. \tag{33}$$

Choose the basis $|i\rangle, i = \{0, \pm 1\}$ in (30) with the ordering of (i, j) such that the ordering of the eigenstates is [(-1,-1),(0,-1), (-1,0), (1,-1), (0,0), (-1,1), (1,0), (0,1), (1,1)]. The Hamiltonian becomes

$$\hat{H}_{\mathrm{BCS},1} = \begin{pmatrix} H_1^{(-2)} & \cdot & \cdot & \cdot & \cdot \\ \cdot & H_1^{(-1)} & \cdot & \cdot & \cdot \\ \cdot & \cdot & H_1^{(0)} & \cdot & \cdot \\ \cdot & \cdot & \cdot & H_1^{(1)} & \cdot \\ \cdot & \cdot & \cdot & \cdot & H_1^{(2)} \end{pmatrix}. \tag{34}$$

Here we identify

$$H_1^{(\pm 2)}(\nu) = 2H_{1/2}^{(\pm 1)}(\nu), \tag{35a}$$

$$H_1^{(-1)}(\nu) = H_{1/2}^{(0)}(\nu/2) - (\varepsilon_1 + \varepsilon_2)\mathbb{I}, \tag{35b}$$

$$H_1^{(1)}(\nu) = H_{1/2}^{(0)}(\nu/2) + \left(\varepsilon_1 + \varepsilon_2 - \frac{1}{\nu t}\right)\mathbb{I}, \tag{35c}$$

$$H_1^{(0)}(\nu) = 2(\epsilon_1 - \epsilon_2)\hat{s}_1^z - \frac{1}{\nu t}\left(2\mathbb{I} + \sqrt{2}\hat{s}_1^x - (\hat{s}_1^z)^2\right). \tag{35d}$$

We notice that the $S^z = \pm 1$ sector, up to a rescaling of ν and an overall (time dependent) term is nothing but the $S^z = 0$ sector from the spin-1/2 model. Then the only novel part that appears in equation (35) is the $S^z = 0$ sector. This sector is identified as the 3×3 hyperbolic Landau-Zener model in equation (10) after using the unitary transformation from Eqs. (19), (20b) and choosing $\Delta = \varepsilon_2 - \varepsilon_1$ with $\varepsilon_2 > \varepsilon_1$.

The prescription outlined above can be carried out for general spin-s and $S^z \neq 0$. More precisely, different magnetization sectors can always be written as a problem of a lower-spin BCS model up to a rescaling of the diabatic energy levels, while the $S^z = 0$ problem introduces additional complexity. As an example of this, we also provide the description of the spin-$3/2$ case in Sec. 4.

On a similar note, one can also consider systems with more than two sites. For instance, the model in (55) is the $S^z = -1/2$ problem of a three-site spin $1/2$ BCS model. One can also find varieties of HLZ problems by tweaking spin representations and site numbers. For the illustration, we consider two and three site BCS models with different spins on each site in Appendix A.

The correspondence between HLZ problems and the KZ equations is an interesting feature, suggesting that solving one problem can help understanding the other. To this end, we wish to make sense of the solution for the LZ problem by means of the contour integral solution of the KZ equations, which we will do in the following subsections. We will specifically solve the contour integral for the spin $1/2$ problem, to show that the resulting wavefunction is indeed the same as that found by direct integration. What is interesting, is that it appears that the choice of the contour defines the boundary conditions of the BCS and therefore the HLZ problems.

3.1.2 Integral representation of the solution of the KZ equations

As mentioned before, the generalised KZ equations (25) have an exact solution via an off-shell Bethe ansatz [13, 22, 25, 26]. For N spins of lengths s_j and the z-projection of the total spin $S^z = M - \sum_j^N s_j$, the solution is given as

$$\Psi(\Omega,\varepsilon) = \oint_\gamma d\lambda \exp\left[-\frac{i\mathcal{S}(\lambda,\varepsilon)}{\nu}\right] |\Phi(\lambda,\varepsilon)\rangle\,, \quad d\lambda = \prod_{\alpha=1}^{M} d\lambda_\alpha, \tag{36}$$

where $\varepsilon = (\varepsilon_1,\ldots,\varepsilon_N)$ with $\varepsilon_1 < \varepsilon_2 < \ldots < \varepsilon_N$, $\lambda = (\lambda_1,\ldots,\lambda_M)$,

$$\begin{aligned}\mathcal{S}(\lambda,\varepsilon) = &-2\Omega\sum_j \varepsilon_j s_j + 2\Omega\sum_\alpha \lambda_\alpha - \frac{1}{2}\sum_j\sum_{j\neq k} s_j s_k \ln(\varepsilon_j - \varepsilon_k),\\ &+\sum_j\sum_\alpha s_j \ln(\varepsilon_j-\lambda_\alpha) - \frac{1}{2}\sum_\alpha\sum_{\beta\neq\alpha}\ln(\lambda_\beta-\lambda_\alpha),\end{aligned} \tag{37}$$

and

$$\Phi \equiv |\Phi(\lambda,\varepsilon)\rangle = \prod_{\alpha=1}^{M} \hat{L}^+(\lambda_\alpha)\,|0\rangle\,, \quad \hat{L}^+ = \sum_{j=1}^{N}\frac{\hat{s}_j^+}{\lambda-\varepsilon_j}. \tag{38}$$

The minimal weight state $|0\rangle$ is the state where all spins point in the negative z-direction, $\hat{s}_j^z\,|0\rangle = -s_j\,|0\rangle$. The closed contour γ is such that the integrand comes back to its initial value after λ_α has described it.

The $s = 1/2$, $S^z = 0$ block of the Hamiltonian[4] (32c) can be solved in the following way. First, the Yang-Yang action (37) takes the explicit form

$$\begin{aligned}\mathcal{S}(\lambda,\epsilon) = &-\nu t(\epsilon_1+\epsilon_2) + 2\nu t\lambda - \frac{1}{4}\log(\epsilon_2-\epsilon_1)\\ &+\frac{1}{2}\log(\epsilon_1-\lambda) + \frac{1}{2}\log(\epsilon_2-\lambda),\end{aligned} \tag{39}$$

where we dropped an imaginary constant that arises when we combine the $\log(\epsilon_2-\epsilon_1)$ and $\log(\epsilon_1-\epsilon_2)$ terms keeping in mind that $\epsilon_2 > \epsilon_1$. This constant is absorbed into the overall normalization factor C independent of t, ϵ_1 and ϵ_2. The state $|\Phi(\lambda,\epsilon)\rangle$ is given by

$$|\Phi(\lambda,\epsilon)\rangle = \prod_\alpha^1 \hat{L}^+(\lambda_\alpha)\,|\downarrow\downarrow\rangle = \frac{1}{\lambda-\epsilon_1}\,|\uparrow\downarrow\rangle + \frac{1}{\lambda-\epsilon_2}\,|\downarrow\uparrow\rangle\,. \tag{40}$$

The solution then becomes

$$\begin{aligned}\Psi(t,\epsilon) = &Ce^{-\frac{i}{\nu}\left[-\nu t(\epsilon_1+\epsilon_2)-\frac{1}{4}\log(\epsilon_2-\epsilon_1)\right]}\times\\ &\oint_\gamma d\lambda e^{-\frac{i}{\nu}\left[2\nu t\lambda+\frac{1}{2}\log(\epsilon_1-\lambda)+\frac{1}{2}\log(\epsilon_2-\lambda)\right]}\left(\frac{1}{\lambda-\epsilon_1}\,|\uparrow\downarrow\rangle + \frac{1}{\lambda-\epsilon_2}\,|\downarrow\uparrow\rangle\right).\end{aligned} \tag{41}$$

This simplifies to

$$\begin{aligned}\Psi(t,\vec{\epsilon}) = Ce^{it(\epsilon_1+\epsilon_2)}(\epsilon_2-\epsilon_1)^{\frac{i}{4\nu}}\Bigg[&\oint_\gamma d\lambda e^{-2it\lambda}(\epsilon_1-\lambda)^{-\frac{i}{2\nu}-1}(\epsilon_2-\lambda)^{-\frac{i}{2\nu}}\,|\uparrow\downarrow\rangle +\\ &\oint_\gamma d\lambda e^{-2it\lambda}(\epsilon_1-\lambda)^{-\frac{i}{2\nu}}(\epsilon_2-\lambda)^{-\frac{i}{2\nu}-1}\,|\downarrow\uparrow\rangle\Bigg].\end{aligned} \tag{42}$$

[4] We note that the 1×1 block can also be solved using the Yang-Yang action, although the result is trivial. For completeness we provide the computation in Appendix B.

We then introduce a new variable η defined by

$$\lambda = \frac{\epsilon_2 + \epsilon_1}{2} - \eta \frac{\epsilon_2 - \epsilon_1}{2}. \tag{43}$$

The integral now becomes

$$\Psi(t,\Delta) = C(\Delta)^{-\frac{3i}{4\nu}} \left[\oint_\gamma d\eta e^{i\eta\Delta t} \frac{(1-\eta^2)^{-\frac{i}{2\nu}}}{1-\eta} |\uparrow\downarrow\rangle - \oint_\gamma d\eta e^{i\eta\Delta t} \frac{(1-\eta^2)^{-\frac{i}{2\nu}}}{1+\eta} |\downarrow\uparrow\rangle \right], \tag{44}$$

where we used $\Delta \equiv (\epsilon_2 - \epsilon_1)$ and collected all constants depending on ν only in the normalization C. Note that there is now a minus sign between the two integrals. Rotating to the same basis as is used in the solution for the differential equation (20a), we reduce the integral to the following form:

$$\begin{aligned}\Psi(t,\Delta) = C(\Delta)^{-\frac{3i}{4\nu}} \sqrt{2} \Bigg[& \oint_\gamma d\eta e^{i\eta\Delta t} \eta \left(\eta^2 - 1\right)^{-\frac{i}{2\nu}-1} |1\rangle + \\ & \oint_\gamma d\eta e^{i\eta\Delta t} \left(\eta^2 - 1\right)^{-\frac{i}{2\nu}-1} |2\rangle \Bigg].\end{aligned} \tag{45}$$

Here, we extracted a overall constant of $(-1)^{-\frac{i}{2\nu}-1} \exp\left[(-\frac{i}{2\nu} - 1)2\pi i r\right]$ for $r \in \mathbb{N}$. This function is multivalued, but since it affects only the overall prefactor, we can safely absorb this term into the normalization constant. For the first integral we use $d\eta = d(\eta^2 - 1)^{-\frac{i}{2\nu}} / \frac{-i\eta}{\nu}(\eta^2 - 1)^{-\frac{i}{2\nu}-1}$. We then integrate by parts and use the fact that the boundary term vanishes. This finally leaves us with

$$\begin{aligned}\Psi(t,\Delta) = C(\Delta)^{-\frac{3i}{4\nu}} \sqrt{2} \Bigg[& \nu t \Delta \oint_\gamma d\eta e^{i\eta\Delta t} \left(\eta^2 - 1\right)^{-\frac{i}{2\nu}} |1\rangle + \\ & \oint_\gamma d\eta e^{i\eta\Delta t} \left(\eta^2 - 1\right)^{-\frac{i}{2\nu}-1} |2\rangle \Bigg].\end{aligned} \tag{46}$$

It turns out that the solution to this integral is given by integral representations of the Bessel function of the first kind as found by Hänkel [45].

As alluded to earlier, the specific choice for the contour determines the initial condition of the system. The contours in question are shown in Figure 4. First, we consider the contour γ_1 in the left of Figure 4, which corresponds to the solution to the differential equation (13) where we started in the ground state. The solution to the integral (46) is then provided using the following result:

$$2\pi i J_\kappa(\tau) = \frac{1}{\sqrt{\pi}} e^{i3\kappa\pi} \left(\frac{\tau}{2}\right)^{-\kappa} \Gamma\left(\kappa + \frac{1}{2}\right) \oint_{\gamma_1} d\eta (\eta^2 - 1)^{-\kappa - \frac{1}{2}} e^{i\eta\tau}. \tag{47}$$

We identify $\tau = t\Delta$, and use $\Gamma(z+1) = z\Gamma(z)$, to write our final answer to the integral (46):

$$|\psi^1_{1/2,0}(\tau)\rangle = C(\Delta)^{-\frac{3i}{4\nu}} i 2^{\frac{i}{2\nu}+2} \frac{\pi^{3/2} \nu \tau^{\frac{i}{2\nu}+\frac{1}{2}}}{e^{-\frac{3}{2\nu}} \Gamma\left(\frac{i}{2\nu}\right)} \left[-i J_{\frac{i}{2\nu}-\frac{1}{2}}(\tau) |1\rangle + J_{\frac{i}{2\nu}+\frac{1}{2}}(\tau) |2\rangle \right]. \tag{48}$$

Indeed, up to normalization this solution is identical to (13).

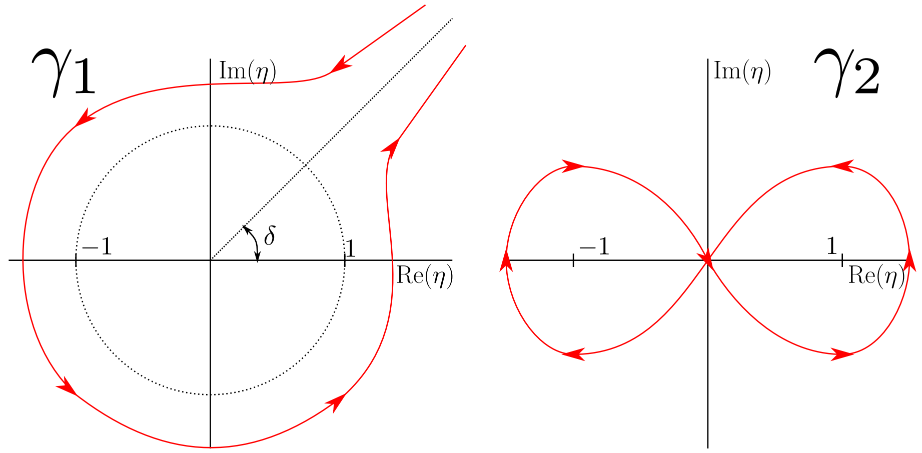

Figure 4: Two choices of the contour to solve equation (46). The red line and arrows draw the path and direction of the contours. The left contour, γ_1 corresponding to (47), encloses the unit circle. The contour is chosen such that $\delta \leq \arg(\eta) \leq 2\pi + \delta$, $-\delta \leq \tau \leq \pi - \delta$ and the values of η range from δ to $\delta + \pi$. For γ_2 corresponding to (49), we only have the requirement that $\kappa + 1/2 \notin \mathbb{N}$

For a different initial condition (i.e. starting in the excited state $|2\rangle$ at $t = 0^+$), one can use the contour γ_2 as given in the right in Figure 4. The integral in this case is solved by using

$$2\pi i J_\kappa(\tau) = \frac{1}{\sqrt{\pi}} \left(\frac{\tau}{2}\right)^\kappa \Gamma\left(\frac{1}{2} - \kappa\right) \oint_{\gamma_2} d\eta (\eta^2 - 1)^{\kappa - \frac{1}{2}} e^{i\eta\tau}. \tag{49}$$

We find

$$|\psi^2_{1/2,0}(\tau)\rangle = C(\Delta)^{-\frac{3i}{4\nu}} \frac{2^{-\frac{i}{2\nu}+2} \pi^{3/2} (-i) \nu \tau^{\frac{i}{2\nu}+\frac{1}{2}}}{\Gamma\left(\frac{i}{2\nu}\right)} \left[i J_{-\frac{i}{2\nu}+\frac{1}{2}}(\tau) |1\rangle + J_{-\frac{i}{2\nu}-\frac{1}{2}}(\tau) |2\rangle \right]. \tag{50}$$

This solution is indeed equal to (16), up to normalization.

3.2 Higher level models and the choice of contour

The calculations in this section show how the HLZ models in Sec. 2 are connected to the KZ equations. For the simplest case, we have explicitly linked the corresponding contour integrals to the solutions that are obtained by directly solving the HLZ problems. This is a promising result, as the choice of the contour appears to dictate the boundary conditions of the HLZ problems. Thus, these HLZ problems reduce to choosing (and solving) the contours for the KZ equations' solution. This choice of contour remains a partially open problem for general HLZ problems. It is not a priori obvious which HLZ initial condition coincides with a arbitrary choice of contour.

For the contour discussed in Fig. 4, one can argue for these shapes by inspecting the stationary points of the Yang-Yang action. The stationary points of the Yang-Yang action (39) can be found readily from the Bethe equation

$$4\nu t = \frac{1}{\varepsilon_1 - \lambda} + \frac{1}{\varepsilon_2 - \lambda}. \tag{51}$$

The solution of this equation in the limits $\nu t \to 0^+$ and $\nu t \to \infty$ are given as

$$\nu t \to 0^+ \ : \begin{cases} \lambda \to -\infty, \\ \lambda \to \frac{\varepsilon_1+\varepsilon_2}{2}, \end{cases} \qquad \nu t \to \infty \ : \begin{cases} \lambda \to \varepsilon_1, \\ \lambda \to \varepsilon_2. \end{cases} \tag{52}$$

The upper row of solutions corresponds to the lowest value for the Bethe root in (51) and the lower two solutions to the highest value for the Bethe root. From the exact solution (37), it can be seen that the evolution is dominated by the stationary points in the $\nu \to 0$ limit, and is adiabatic. Therefore, in order to start in the ground state with the lowest value for the Bethe root at $t = 0^+$, we presumably need a contour that can be pushed onto the point $\lambda = -\infty$, but not the point $\lambda = \frac{\varepsilon_1+\varepsilon_2}{2}$ and vice versa for when the initial condition is the excited state. This argument can be made directly for the integrals solved in this section, however it is not immediately clear how to generalize it for more complicated integral solutions to the LZ problems.

We also point out a interesting example of a complicated integral structure that is found in the two-site spin-1 BCS Hamiltonian. Specifically, the Yang-Yang action corresponding to the H_1^0 sector in (35d) is written as

$$\begin{aligned} \mathcal{S}_{H_1^0}(\vec{\lambda},\vec{\epsilon}) = & -2\nu t(\epsilon_1+\epsilon_2)+2\nu t(\lambda_1+\lambda_2)-\log(\epsilon_2-\epsilon_1)+\log(\epsilon_1-\lambda_1) \\ & +\log(\epsilon_2-\lambda_1)+\log(\epsilon_1-\lambda_2)+\log(\epsilon_2-\lambda_2)-\log(\lambda_2-\lambda_1). \end{aligned} \tag{53}$$

Here, there are two integration variables, λ_1 and λ_2. This means that the solution as given by the Yang-Yang action (37) is a double contour integral. Unfortunately, we have not been able to perform this integral explicitly. However, from the corresponding HLZ problem we know that the following must hold:

$$U \oint_\gamma d\vec{\lambda} \exp\left[-\frac{i\mathcal{S}_{H_1^0}(\vec{\lambda},\vec{\varepsilon})}{\nu}\right] |\Phi(\vec{\lambda},\vec{\varepsilon})\rangle \propto |\psi_{1,0}^k(\tau)\rangle\,, \tag{54}$$

where $\vec{\varepsilon} = (\epsilon_1, \epsilon_2)$, $\vec{\lambda} = (\lambda_1, \lambda_2)$, $|\psi_{1,0}^k(\tau)\rangle$ is given in (17) and U is the unitary transformation as defined by (19) and (20b). The contours γ in (54) determine which state $|\psi_{1,0}^k(\tau)\rangle$ is computed. We speculate that the choices for γ are double contours comprised of the ones shown in Figure 4.

For example, we expect the boundary condition where the HLZ problem (10) starts in the ground state (15) to be associated with the contour γ_1 in Figure 4 with a second contour of the same shape enveloping the first. Starting in the first excited state then corresponds to γ_1 enveloping γ_2 with the final boundary condition being given by a double γ_2 contour. We find that the number of possible combinations of the two contours given in Figure 4 equals the number of boundary conditions for any spin-s two-site BCS model-derived HLZ problem. For larger-site ($N > 2$) BCS models this no longer holds, due to the additional branch points that appear in the integral-solution to the corresponding KZ equation. The appropriate contours for these HLZ models are a topic of further investigation.

In the next section, we will consider several other models, that, according to the KZ prescription are integrable, but for which no solutions in terms of known functions currently exists.

4 New 3 × 3 and 4 × 4 integrable HLZ models

With the connection between the KZ equations and LZ models established, we now proceed to discuss two more examples of HLZ models that derive from the time dependent BCS Hamiltonian (28). Furthermore, we will also make more general statements on higher order HLZ problems. Due to their connection to the KZ equations, all these models are integrable, yet we will obtain exact solutions to some of them.

4.1 Three-site spin-1/2 BCS-derived HLZ problem

First, we consider a problem derived from the three-site spin-$1/2$ BCS Hamiltonian. It is found within the $S^z = -1/2$ sector, see equation (A.24). It looks similar to equation (10) and is described by

$$i\begin{pmatrix}\dot{\psi}_1(t)\\ \dot{\psi}_2(t)\\ \dot{\psi}_3(t)\end{pmatrix} = \begin{pmatrix}\frac{\alpha\Delta}{3}-\frac{3}{2\nu t} & \sqrt{\frac{2}{3}}\Delta & -\frac{1}{3}\sqrt{2}\alpha\Delta\\ \sqrt{\frac{2}{3}}\Delta & \frac{2\alpha\Delta}{3} & -\frac{\Delta}{\sqrt{3}}\\ -\frac{1}{3}\sqrt{2}\alpha\Delta & -\frac{\Delta}{\sqrt{3}} & 0\end{pmatrix}\begin{pmatrix}\psi_1(t)\\ \psi_2(t)\\ \psi_3(t)\end{pmatrix}, \tag{55}$$

where $-1 \leq \alpha \leq 1$ and Δ and ϵ_1 are positive real numbers.

For $\alpha = 0$, the model reduces to the form (10) with parameters given as

$$\left\{p = -\frac{3}{2\nu},\ q = 0,\ a_1 = \sqrt{\frac{2}{3}}\Delta,\ a_2 = -\frac{\Delta}{\sqrt{3}}\right\}. \tag{56}$$

This problem is solved in general in Appendix A.4 in terms of the ${}_1F_2$ hypergeometric functions. To make sense of this problem as one may derive it from a magnetization sector the BCS Hamiltonian, we make the following identification for the basis states of the spin-$1/2$ particles:

$$\begin{aligned}|1\rangle &= \frac{1}{\sqrt{3}}(|\uparrow\downarrow\downarrow\rangle + |\downarrow\uparrow\downarrow\rangle + |\downarrow\downarrow\uparrow\rangle),\\ |2\rangle &= \frac{1}{\sqrt{2}}(-|\uparrow\downarrow\downarrow\rangle + |\downarrow\downarrow\uparrow\rangle),\\ |3\rangle &= \frac{1}{\sqrt{6}}(-|\uparrow\downarrow\downarrow\rangle + 2|\downarrow\uparrow\downarrow\rangle - |\downarrow\downarrow\uparrow\rangle).\end{aligned} \tag{57}$$

The probability transition matrix is calculated to be

$$P_{3\times3} = \begin{pmatrix}\frac{e^{\frac{\pi}{\nu}}}{1+2\cosh\left(\frac{\pi}{\nu}\right)} & \frac{1}{1+2\cosh\left(\frac{\pi}{\nu}\right)} & \frac{1}{1+e^{\frac{\pi}{\nu}}+e^{\frac{2\pi}{\nu}}}\\ \frac{1}{2\left(1+e^{\frac{\pi}{\nu}}-e^{\frac{\pi}{2\nu}}\right)} & \frac{\left(e^{\frac{\pi}{2\nu}}-1\right)^2}{2\left(1+e^{\frac{\pi}{\nu}}-e^{\frac{\pi}{2\nu}}\right)} & \frac{e^{\frac{\pi}{\nu}}}{2\left(1+e^{\frac{\pi}{\nu}}-e^{\frac{\pi}{2\nu}}\right)}\\ \frac{1}{2\left(1+e^{\frac{\pi}{\nu}}+e^{\frac{\pi}{2\nu}}\right)} & \frac{1}{2}+\frac{1}{2(1+2\cosh[\frac{\pi}{2\nu}])} & \frac{e^{\frac{\pi}{\nu}}}{2\left(1+e^{\frac{\pi}{\nu}}+e^{\frac{\pi}{2\nu}}\right)}\end{pmatrix}. \tag{58}$$

A plot of the transition probabilities and the energy spectrum as a function of time is provided in Figure 5.

By tuning the value of α to 1 or -1, a non-trivial degeneracy arises at $t \to \infty$, see Appendix A.5. Here, the middle energy band coalesces with either the ground state or the highest band respectively. While the differential equations can be solved for certain choices of boundary conditions, they are unfortunately not sufficient to compute the probability transition matrix. More details are provided in Appendix A.5 with plots of numerical simulation for the case of $\alpha = -1$ given in Figure 8.

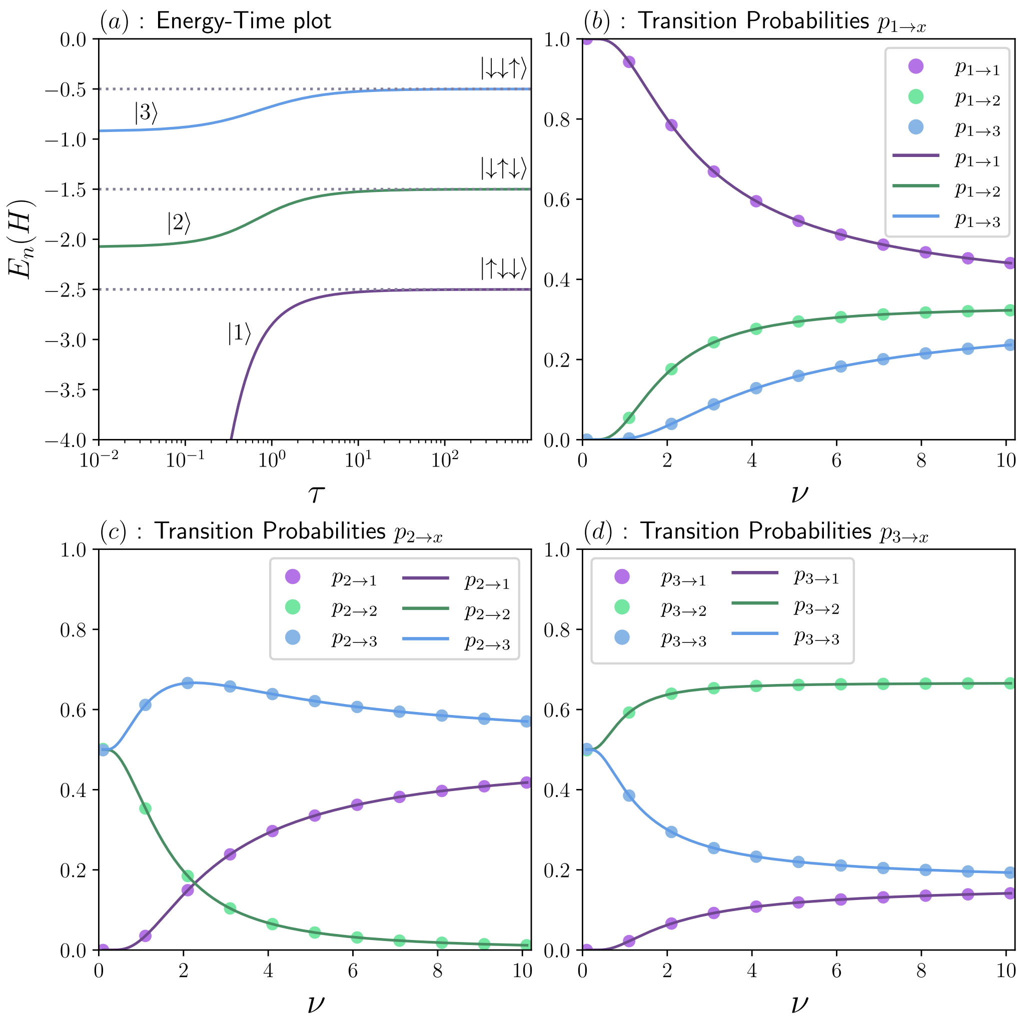

Figure 5: (a) Instantaneous eigenvalues of the 3×3 HLZ model (56) vs $\tau = t\Delta$ for $\nu = 2$. The ground state $|1\rangle$ evolves towards $|\uparrow\downarrow\downarrow\rangle$ (purple curve). $|2\rangle$ and $|3\rangle$ evolve to $|\downarrow\uparrow\downarrow\rangle$ (green curve) and $|\downarrow\downarrow\uparrow\rangle$ (blue curve) respectively. (b–d) Elements of the transition probability matrices, where the solid lines represent the analytical expressions in (24). The scatter plots represent the numerical simulation of $p_{x\to y}$ as a function of ν at $\tau = 10^3$.

4.2 Two-site spin-3/2 BCS-derived HLZ problem

Here we consider a HLZ problem that is derived from a spin-3/2 BCS Hamiltonian. We introduce the spin-3/2 operators,

$$\hat{s}^z_{3/2} = \frac{1}{2}\begin{pmatrix} 3 & 0 & 0 & 0 \\ 0 & 1 & 0 & 0 \\ 0 & 0 & -1 & 0 \\ 0 & 0 & 0 & -3 \end{pmatrix}, \quad \hat{s}^+_{3/2} = \begin{pmatrix} 0 & \sqrt{3} & 0 & 0 \\ 0 & 0 & 2 & 0 \\ 0 & 0 & 0 & \sqrt{3} \\ 0 & 0 & 0 & 0 \end{pmatrix}, \quad \hat{s}^-_{3/2} = \begin{pmatrix} 0 & 0 & 0 & 0 \\ \sqrt{3} & 0 & 0 & 0 \\ 0 & 2 & 0 & 0 \\ 0 & 0 & \sqrt{3} & 0 \end{pmatrix}. \tag{59}$$

We write the wavefunctions in the canonical basis states $|i\rangle, i = \pm 1, \pm 3$ as in (30) where $|i\rangle$ is the eigenstate of $\hat{s}^z_{3/2}$ with eigenvalue $i/2$. By ordering the (i,j) indices as

$$\begin{aligned}&[(-3,-3),\\ &(-1,-3),(-3,-1),\\ &(1,-3),(-1,-1),(-3,1),\\ &(3,-3),(1,-1),(-1,1),(-3,3),\\ &(3,-1),(1,1),(-1,3),\\ &(3,1),(1,3),\\ &(3,3)]\end{aligned} \tag{60}$$

we find

$$\hat{H}_{\mathrm{BCS},3/2} = \bigoplus_{S^z=-3}^{3} H^{(S^z)}_{3/2}, \tag{61}$$

where

$$\begin{aligned}
H^{(\pm 3)}_{3/2}(\nu) &= 3H^{(\pm 1)}_{1/2}(\nu),\\
H^{(-2)}_{3/2}(\nu) &= H^{(0)}_{1/2}(\nu/3) - 2(\varepsilon_1+\varepsilon_2)\mathbb{I},\\
H^{(2)}_{3/2}(\nu) &= H^{(0)}_{1/2}(\nu/3) + 2\left(\varepsilon_1+\varepsilon_2 - \frac{1}{\nu t}\right)\mathbb{I},\\
H^{(-1)}_{3/2}(\nu) &= H^{(0)}_{1}(\nu/\sqrt{3}) + (\varepsilon_1+\varepsilon_2)\mathbb{I} - \frac{1}{\nu t}\mathrm{diag}(2-\sqrt{3}, 3-2\sqrt{3}, 2-\sqrt{3}),\\
H^{(1)}_{3/2}(\nu) &= H^{(0)}_{1}(\nu/\sqrt{3}) + (\varepsilon_1+\varepsilon_2)\mathbb{I} - \frac{1}{\nu t}\mathrm{diag}(3-\sqrt{3}, 4-2\sqrt{3}, 3-\sqrt{3}).
\end{aligned} \tag{62}$$

It is worth noting that we cannot solve for $H^{(\pm 1)}_{3/2}$ through any re-scaling of the $S^z = 0$ solution of the spin-1 case. This is because in this case, the Hamiltonian is not shifted by a term proportional to unity as before, but rather the individual (adiabatic) energy levels have shifted. Since the equations are still fundamentally the same, the solution to this problem is given in terms of the ${}_1F_2$ hypergeometric functions (see Appendix A.4).

The $S^z = 0$ sector is written using the spin-3/2 (59) operators as

$$\begin{aligned}
H^{(0)}_{3/2}(\nu) = 2(\varepsilon_1-\varepsilon_2)\hat{s}^z_{3/2} - \frac{1}{\nu t}\Bigg[&\frac{1}{2}\left(\hat{s}^+_{3/2}\cdot\hat{s}^-_{3/2} + \hat{s}^-_{3/2}\cdot\hat{s}^+_{3/2}\right)\\
&+\left(\frac{3}{2}-2\sqrt{3}\right)\left(\hat{s}^+_{3/2}\cdot\hat{s}^+_{3/2}\cdot\hat{s}^-_{3/2} + \hat{s}^-_{3/2}\cdot\hat{s}^-_{3/2}\cdot\hat{s}^+_{3/2}\right)\\
&+\left(3\sqrt{3}-2\right)\left(\hat{s}^+_{3/2}\cdot\hat{s}^-_{3/2}\cdot\hat{s}^+_{3/2} + \hat{s}^-_{3/2}\cdot\hat{s}^+_{3/2}\cdot\hat{s}^-_{3/2}\right)\\
&+\left(\frac{3}{2}-2\sqrt{3}\right)\left(\hat{s}^-_{3/2}\cdot\hat{s}^+_{3/2}\cdot\hat{s}^+_{3/2} + \hat{s}^+_{3/2}\cdot\hat{s}^-_{3/2}\cdot\hat{s}^-_{3/2}\right)\Bigg].
\end{aligned} \tag{63}$$

The solution of the non-stationary Schrödinger equation for this Hamiltonian is out of reach for the present work.

4.2.1 A new 4×4 integrable HLZ model and remarks on $N > 4$ integrable models

While we do not attempt to fully solve the non-stationary Schrödinger equation for the $H^{(0)}_{3/2}$ block in equation (63), we do solve the corresponding 4×4 HLZ problem numerically. Here we also provide some remarks on the general multi-state problems that can be constructed by going to higher spin-s representations.

First, it is interesting to note that (20a) and (20b) are also the eigenstates of $\hat{S}^+\hat{S}^- = \sum_{j,k}\hat{s}_j^+\hat{s}_k^-$ in their corresponding spin representation. By choosing the correct eigenstates of $\hat{S}^+\hat{S}^-$ of a given S^z sector, we can construct the unitary transformation to simplify $H^{(S^z)}$ blocks of arbitrary spin-s. For instance, for $S^z = 0$ this allows us to define the following orthogonal transformation:

$$\begin{aligned} |3/2,0\rangle_g \equiv |1\rangle &= \frac{1}{2\sqrt{5}}\left(|3,\text{-}3\rangle + 3\,|1,\text{-}1\rangle + 3\,|\text{-}1,1\rangle + |\text{-}3,3\rangle\right), \\ |2\rangle &= \frac{1}{2}\left(-|3,\text{-}3\rangle - |1,\text{-}1\rangle + |\text{-}1,1\rangle + |\text{-}3,3\rangle\right), \\ |3\rangle &= \frac{1}{2\sqrt{5}}\left(3\,|3,\text{-}3\rangle - |1,\text{-}1\rangle - |\text{-}1,1\rangle + 3\,|\text{-}3,3\rangle\right), \\ |4\rangle &= \frac{1}{2}\left(-|3,\text{-}3\rangle + |1,\text{-}1\rangle - |\text{-}1,1\rangle + |\text{-}3,3\rangle\right). \end{aligned} \tag{64}$$

Then, the differential equation of $H^{(0)}_{3/2}$ takes the form

$$i\begin{pmatrix}\dot{\psi}_1(t)\\ \dot{\psi}_2(t)\\ \dot{\psi}_3(t)\\ \dot{\psi}_4(t)\end{pmatrix} = \begin{pmatrix} -\frac{6}{\nu t} & \frac{3\Delta}{\sqrt{5}} & 0 & 0 \\ \frac{3\Delta}{\sqrt{5}} & -\frac{3}{\nu t} & \frac{4\Delta}{\sqrt{5}} & 0 \\ 0 & \frac{4\Delta}{\sqrt{5}} & -\frac{1}{\nu t} & \sqrt{5}\Delta \\ 0 & 0 & \sqrt{5}\Delta & 0 \end{pmatrix}\begin{pmatrix}\psi_1(t)\\ \psi_2(t)\\ \psi_3(t)\\ \psi_4(t)\end{pmatrix}, \tag{65}$$

where $\Delta = \varepsilon_1 - \varepsilon_2$. All HLZ models in this work are presented as tridiagonal matrices, with only the diagonal elements being time dependent as $\propto 1/t$. In fact, this is the general appearance of any $N \times N$ representation of our model. The plots of instantaneous (adiabatic) eigenvalues of these models also have a familiar behaviour: at $t = 0^+$, the BCS ground state evolves from the lowest energy, while the highest energy band begins at $E = 0$. At $t \to \infty$, they all tend towards one of the $|i\rangle \otimes |j\rangle$ states, see Figure 6.

Finally, it is always possible to identify the transition probabilities at the limits $\nu \to 0$ (adiabatic, assuming there are no degeneracy) and $\nu \to \infty$ (diabatic). In the adiabatic limit, $p_{x\to x} = 1$, while the remaining probabilities are zero. In the diabatic limit, each $p_{x\to y}$ is given by the weighted coefficients of the basis transformation in (64). We numerically validate this in Figure 7 (the grey dashed lines) for $s = 3/2$, and it can be further verified with the help of (22) and (24). Additionally, using a saddle-point approach, one can always compute each $p_{1\to y}$ [5] as was done in [32].

[5] Here the label '1' refers to the BCS ground state of each magnetization sector in the BCS Hamiltonian.

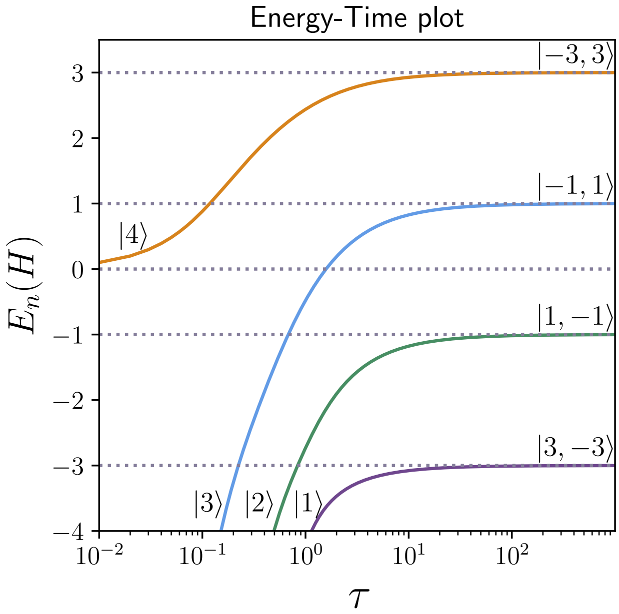

Figure 6: Instantaneous eigenvalues of $H^{(0)}_{3/2}$ as functions of time $\tau = t\Delta$ for $\varepsilon_1 = 1$, $\varepsilon_2 = 2$, and $\nu = 2$. The BCS ground state $|1\rangle$ evolves towards $|3,\text{-}3\rangle$ which represents the lowest energy curve.

5 Conclusion & Discussion

In this work, we obtained exact solutions for several hyperbolic Landau-Zener (HLZ) problems. We solved a number of nontrivial examples of the non-stationary Schrödinger equation of the form $i\frac{\partial\Psi}{\partial t} = (A + B/t)\Psi$, where A and B are time-independent $N \times N$ Hermitian matrices. We obtained the wavefunctions $\Psi(t)$ at arbitrary time t as well as transition probabilities between eigenstates at $t = 0^+$ and $t \to +\infty$. More importantly, we demonstrated how these models arise from the generalized Knizhnik-Zamolodchikov (KZ) equations of Conformal Field Theory.

The BCS Hamiltonian with the superconducting coupling parameter inversely proportional to time shares the integrability properties of the KZ equations. By examining individual magnetization sectors in the finite-size BCS model, we readily identified a plethora of integrable HLZ problems, some of which we explicitly solved as mentioned above. Meanwhile, the KZ equations are solvable in terms of (multidimensional) contour integrals. We explicitly showed how the choice of the contours determines the boundary conditions of the corresponding HLZ problem. We suggest that most, if not all, solvable finite-dimensional Landau-Zener problems are connected to the KZ theory (including various generalisations of the KZ equations) in the manner described in this work.

There are several intriguing problems that remain unsolved. One is the general solution of the 3×3 problem (A.20), which itself is a generalisation of (10). Another problem is to identify the proper contours and to compute the integral in the solution of the KZ equations (54) corresponding to the spin-1 derived 3×3 HLZ problem. A similar 3×3 problem derived from a three-site spin-$1/2$ BCS Hamiltonian, which we solved in terms of generalised hypergeometric functions in Section 4.1, can also be written in terms of contour integrals. Finally, we note that (55) for $\alpha = \pm 1$ represents a 3-site BCS problem with degenerate single-particle energy levels (Zeeman fields) ϵ_j. While this problem can be solved for certain boundary conditions,

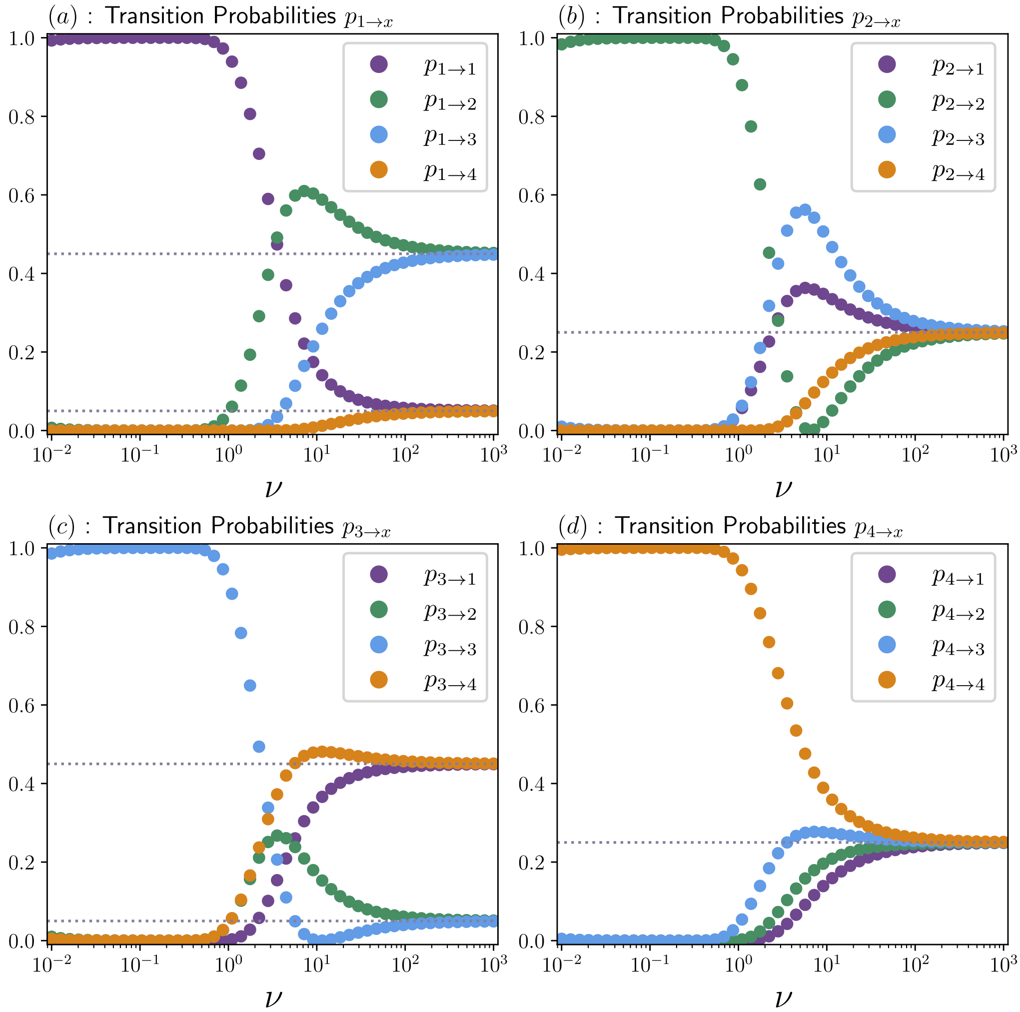

Figure 7: (a – d) Numerically evaluated transition probabilities $p_{x\to y}$ for the 4×4 HLZ model at $\tau=10^3$ as functions of ν at log-equidistant values between 10^{-2} and 10^3. Gray horizontal lines indicate the predicted probabilities from (64) : in (a),(c) they are $1/20$ and $9/20$ and in (b),(d) it is $1/4$. At large ν, the expected behaviour of $p_{x\to y}$ is verified. For $\nu\approx0$, $p_{x\to x}$ tends towards unity, while the rest of probabilities are approximately 0.

the evolution starting from the ground state at $t=0^+$ is still unknown. This will be investigated in further work. In general, we believe that in order to systematically solve the contour integration problems described in this manuscript, cohomology methods should be employed.

As a final note, we emphasize that all models presented in this work are solely based on the the $su(2)$ algebra. Generalizations to other Lie algebras should reveal new classes of integrable (H)LZ models. This is reserved as a topic for later investigation.

Acknowledgements

The authors thank Gor Sarkissian, Jean-Sébastien Caux and Mikhail Isachenkov for helpful discussions and references.

Code availability All code used to create the figures and derive results is readily available in a publicly accessible code repository [46].

Funding information The work of SB and VG is partially supported by the Delta Institute for Theoretical Physics (DITP). The DITP consortium, a program of the Netherlands Organization for Scientific Research (NWO), is funded by the Dutch Ministry of Education, Culture and Science (OCW). The authors also thank the Delta Institute for Theoretical Physics and the Institute of Physics at the University of Amsterdam for graciously hosting EY, which ultimately resulted in this work.

A Derivation of HLZ models from the KZ-BCS theory

In this section, we will show step-by-step how we arrive at HLZ problems from an n-site BCS Hamiltonian for spins of magnitude j_i. The Hamiltonian reads

$$H = 2\sum_{i=1}^{n} \epsilon_i \hat{s}_i^z - \frac{1}{2\nu t}\left(\sum_{i=1}^{n} \hat{s}_i^+\right)\left(\sum_{i=1}^{n} \hat{s}_i^-\right), \tag{A.1}$$

where $s_i^z |j_i, m\rangle = m\, |j_i, m\rangle$ and $s_i^\pm |j_i, m\rangle = \sqrt{j_i(j_i+1) - m(m\pm 1)}\, |j_i, m\pm 1\rangle$.

A.1 The 2 × 2 case

For $n = 2$, we look into the $S^z = -j_1 - j_2 + 1$ sector, whose basis states are given by

$$|b_i\rangle = \bigotimes_{j=1}^{2} |j_i, -j_i + \delta_{i,j}\rangle\,,\; i = 1, 2. \tag{A.2}$$

Investigating the matrix elements of the Hamiltonian in this basis, we determine the corresponding block

$$H_{2\times 2}^{j_1,j_2} = -2\sum_{i=1}^{2} \epsilon_i j_i \mathbb{I} + 2\begin{pmatrix} \epsilon_1 & 0 \\ 0 & \epsilon_2 \end{pmatrix} - \frac{1}{\nu t}\begin{pmatrix} j_1 & \sqrt{j_1 j_2} \\ \sqrt{j_2 j_1} & j_2 \end{pmatrix}. \tag{A.3}$$

Using the unitary transformation

$$T = \frac{1}{\sqrt{j_1 + j_2}}\begin{pmatrix} \sqrt{j_1} & \sqrt{j_2} \\ -\sqrt{j_2} & \sqrt{j_1} \end{pmatrix}, \tag{A.4}$$

we rewrite the Hamiltonian as

$$H_{2\times 2}^{LZ} = 2\begin{pmatrix} -\frac{j_1+j_2}{2\nu t} - \left(\frac{j_1-j_2}{j_1+j_2}\right)(\epsilon_2 - \epsilon_1) & (\epsilon_2 - \epsilon_1) \\ (\epsilon_2 - \epsilon_1) & 0 \end{pmatrix} \tag{A.5}$$

up to a multiple of identity $\left[\frac{2(j_2\epsilon_1 + j_1\epsilon_2)}{j_1+j_2} - 2\sum_{i=1}^{2} \epsilon_i j_i\right]\mathbb{I}$. This model is of the form (8). Taking $j_1 = j_2$, we reproduce the parameterization (9) that we considered in the main text.

A.2 Solution to the 2 × 2 case

Consider the following set of differential equations

$$i\begin{pmatrix}\dot{\phi}_1(t)\\ \dot{\phi}_2(t)\end{pmatrix}=\begin{pmatrix}\frac{p}{t}+a_1 & a_2\\ a_2 & 0\end{pmatrix}\begin{pmatrix}\phi_1(t)\\ \phi_2(t)\end{pmatrix} \tag{A.6}$$

where $a_1 \neq 0$. The case with $a_1 = 0$ is solved in the main text. Eliminating ϕ_1 from the first equation, we obtain

$$\ddot{\phi}_2(t)+i\left(\frac{p}{t}+a_1\right)\dot{\phi}_2(t)+a_2^2\phi_2(t)=0, \tag{A.7}$$

$$\frac{i}{b}\dot{\phi}_2(t)=\phi_1(t). \tag{A.8}$$

The solution of (A.7) is

$$\begin{aligned}\phi_2(t)=&\mathcal{C}_1 e^{-\frac{1}{2}(\mu+ia_1)t}U\left(\frac{1}{2}p\left(i-\frac{a_1}{\mu}\right),ip,t\mu\right)\\ &+\mathcal{C}_2 e^{-\frac{1}{2}(\mu+ia_1)t}L^{ip-1}_{\frac{1}{2}p\left(-i+\frac{a_1}{\mu}\right)}(t\mu),\end{aligned} \tag{A.9}$$

where $\mu=\sqrt{-a_1^2-4a_2^2}$. U and L are the Tricomi Hypergeometric and Generalised Laguerre functions respectively. $\mathcal{C}_{1,2}$ are arbitrary complex constants which fix the boundary condition.

A.3 The 3 × 3 cases

For $n=3$, we are interested in the $S^z=-j_1-j_2-j_3+1$ sector. The basis states are

$$|b_i\rangle=\bigotimes_{j=1}^{3}|j_i,-j_i+\delta_{i,j}\rangle,\; i=1,2,3. \tag{A.10}$$

In this basis,

$$H^{j_1,j_2,j_3}_{3\times 3}=-2\sum_{i=1}^{3}\epsilon_i j_i\mathbb{I}+2\begin{pmatrix}\epsilon_1&0&0\\0&\epsilon_2&0\\0&0&\epsilon_3\end{pmatrix}-\frac{1}{\nu t}\begin{pmatrix}j_1&\sqrt{j_1j_2}&\sqrt{j_1j_3}\\ \sqrt{j_2j_1}&j_2&\sqrt{j_2j_3}\\ \sqrt{j_3j_1}&\sqrt{j_3j_2}&j_3\end{pmatrix}. \tag{A.11}$$

We use the following unitary transformation

$$T=\begin{pmatrix}\sqrt{\frac{j_1}{j_1+j_2+j_3}}&\sqrt{\frac{j_2}{j_1+j_2+j_3}}&\sqrt{\frac{j_3}{j_1+j_2+j_3}}\\ -\sqrt{\frac{j_2}{j_1+j_2}}&\sqrt{\frac{j_1}{j_1+j_2}}&0\\ -\sqrt{\frac{j_1j_3}{(j_1+j_2)(j_1+j_2+j_3)}}&\sqrt{\frac{j_2j_3}{(j_1+j_2)(j_1+j_2+j_3)}}&\sqrt{\frac{j_1+j_2}{j_1+j_2+j_3}}\end{pmatrix} \tag{A.12}$$

and choose

$$\epsilon_2=\frac{j_1(\epsilon_3-\epsilon_1)}{j_2}+\epsilon_3. \tag{A.13}$$

Then, the transformed model takes the form

$$H^{LZ}_{3\times 3}=2\begin{pmatrix}-\frac{j_1+j_2+j_3}{2\nu t}&\sqrt{\frac{j_1(j_1+j_2)}{j_2(j_1+j_2+j_3)}}(\epsilon_1-\epsilon_3)&0\\ \sqrt{\frac{j_1(j_1+j_2)}{j_2(j_1+j_2+j_3)}}(\epsilon_1-\epsilon_3)&\left(\frac{j_1}{j_2}-1\right)(\epsilon_3-\epsilon_1)&\sqrt{\frac{j_1j_3}{j_2(j_1+j_2+j_3)}}(\epsilon_1-\epsilon_3)\\ 0&\sqrt{\frac{j_1j_3}{j_2(j_1+j_2+j_3)}}(\epsilon_1-\epsilon_3)&0\end{pmatrix}, \tag{A.14}$$

up to a multiple of identity $\left(2\epsilon_3 - 2\sum_{i=1}^{3}\epsilon_i j_i\right)\mathbb{I}$.

The Hamiltonian (A.14) is a new integrable HLZ model and can be generically written as

$$H^{LZ}_{3\times3} = \begin{pmatrix} \frac{p}{t} & a_1 & 0 \\ a_1 & a_3 & a_2 \\ 0 & a_2 & 0 \end{pmatrix}, \tag{A.15}$$

with arbitrary real parameters a_1, a_2, a_3, and p. So far, we have not found an analytical solution to the non-stationary Schrödinger equation for this model. For $j_1 = j_2$, (A.14) takes the form of (10) with $q = 0$. The solution presented in Appendix A.4 for the 3×3 model solves the $S^z = -j_1 - j_2 - j_3 + 1$ sector of the three-site BCS model with on-site Zeeman fields $(\epsilon_1, \frac{1}{2}(\epsilon_1+\epsilon_3), \epsilon_3)$.

We can also arrive to a 3×3 problem from the $n = 2$ BCS Hamiltonian. Consider the sector $S^z = -j_1 - j_2 + 2$ where $j_1, j_2 > 1/2$. The basis states are

$$|b_{n,m}\rangle = \bigotimes_{j=1}^{2} |j_i, -j_i + \delta_{n,j} + \delta_{m,j}\rangle\,,\; n, m \in \{1,2\}. \tag{A.16}$$

Choosing the basis ordering as $\left(b_{1,1}, b_{1,2}, b_{2,2}\right)$, we write the matrix elements as

$$\begin{aligned} H^{j_1,j_2}_{3\times3} = &-2\sum_{i=1}^{2}\epsilon_i j_i \mathbb{I} + 2\begin{pmatrix} 2\epsilon_1 & 0 & 0 \\ 0 & \epsilon_1+\epsilon_2 & 0 \\ 0 & 0 & 2\epsilon_2 \end{pmatrix} \\ &-\frac{1}{\nu t}\begin{pmatrix} 2j_1+1 & \sqrt{(2j_1+1)j_2} & 0 \\ \sqrt{(2j_1+1)j_2} & j_1+j_2 & \sqrt{(2j_2+1)j_1} \\ 0 & \sqrt{(2j_2+1)j_1} & 2j_2+1 \end{pmatrix}. \end{aligned} \tag{A.17}$$

The unitary transformation involved is

$$T = \begin{pmatrix} \sqrt{\frac{j_1(2j_1+1)}{(j_1+j_2)(2j_1+2j_2+1)}} & 2\sqrt{\frac{j_1 j_2}{(j_1+j_2)(2j_1+2j_2+1)}} & \sqrt{\frac{j_2(2j_2+1)}{(j_1+j_2)(2j_1+2j_2+1)}} \\ -\sqrt{\frac{(2j_1+1)j_2}{(j_1+j_2)(j_1+j_2+1)}} & \frac{j_1-j_2}{\sqrt{(j_1+j_2)(j_1+j_2+1)}} & \sqrt{\frac{j_1(2j_2+1)}{(j_1+j_2)(j_1+j_2+1)}} \\ \sqrt{\frac{j_2(2j_2+1)}{(j_1+j_2+1)(2j_1+2j_2+1)}} & -\sqrt{\frac{(2j_1+1)(2j_2+1)}{(j_1+j_2+1)(2j_1+2j_2+1)}} & \sqrt{\frac{j_1(2j_1+1)}{(j_1+j_2+1)(2j_1+2j_2+1)}}. \end{pmatrix} \tag{A.18}$$

We then write

$$\begin{aligned} H^{LZ}_{3\times3,(2)} = &2(\epsilon_2-\epsilon_1)\begin{pmatrix} \frac{(j_2-j_1)(2j_1+2j_2+1)}{(j_1+j_2)(j_1+j_2+1)} & 2\sqrt{\frac{j_1 j_2(j_1+j_2+1)}{(2j_1+2j_2+1)(j_1+j_2)^2}} & 0 \\ 2\sqrt{\frac{j_1 j_2(j_1+j_2+1)}{(2j_1+2j_2+1)(j_1+j_2)^2}} & \frac{(j_2-j_1)(j_1+j_2-1)}{(j_1+j_2)(j_1+j_2+1)} & \sqrt{\frac{(2j_1+1)(j_1+j_2)(2j_2+1)}{(2j_1+2j_2+1)(j_1+j_2+1)^2}} \\ 0 & \sqrt{\frac{(2j_1+1)(j_1+j_2)(2j_2+1)}{(2j_1+2j_2+1)(j_1+j_2+1)^2}} & 0 \end{pmatrix} \\ &-\frac{1}{\nu t}\begin{pmatrix} 2j_1+2j_2+1 & 0 & 0 \\ 0 & j_1+j_2+1 & 0 \\ 0 & 0 & 0 \end{pmatrix} + 2\left(\frac{2j_2\epsilon_1+2j_1\epsilon_2+\epsilon_1+\epsilon_2}{j_1+j_2+1} - \sum_{i=1}^{2}\epsilon_i j_i\right)\mathbb{I}. \end{aligned} \tag{A.19}$$

Thus, we arrive to a generalisation of the model which can be summarized as

$$H^{LZ}_{3\times3} = \begin{pmatrix} \frac{p}{t}+a_3 & a_1 & 0 \\ a_1 & \frac{q}{t}+a_4 & a_2 \\ 0 & a_2 & 0 \end{pmatrix}, \tag{A.20}$$

with arbitrary real $a_{1,2,3}$, p, and q. Thus far we have not been able to identify the general solution to this problem. Setting $j_1 = j_2$, we obtain (10). Appendix A.4 also solves the $S^z = -2j+1$ sector of the two-site BCS model with spins of the same magnitude j for arbitrary, distinct on-site Zeeman fields ϵ_1 and ϵ_2.

A.4 Solution to 3 × 3 cases

Consider the following set of differential equations

$$i\begin{pmatrix}\dot{\phi}_1(t)\\ \dot{\phi}_2(t)\\ \dot{\phi}_3(t)\end{pmatrix}=\begin{pmatrix}\frac{p}{t} & a_1 & 0\\ a_2 & \frac{q}{t} & a_3\\ 0 & a_4 & 0\end{pmatrix}\begin{pmatrix}\phi_1(t)\\ \phi_2(t)\\ \phi_3(t)\end{pmatrix}. \tag{A.21}$$

These equations are a generalised version of (10), but a special case of (A.20). These differential equations can be cast into the form

$$\begin{aligned}&-it^3\dddot{\phi}_1(t)+(p+q)t^2\ddot{\phi}_1(t)+\left(ipq-2p-q-i(a_4a_3+a_2a_1)t^2\right)t\dot{\phi}_1(t)\\&+p\left(-2iq+t^2a_3a_4+2\right)\phi_1(t)=0,\end{aligned} \tag{A.22a}$$

$$\phi_2(t)=\frac{1}{a_1}\left[i\dot{\phi}_1(t)-\frac{p}{t}\phi_1(t)\right], \tag{A.22b}$$

$$\phi_3(t)=\frac{1}{a_1a_3}\left[-\ddot{\phi}_1(t)-\frac{i}{t}(p+q)\dot{\phi}_1(t)+\frac{1}{t^2}(p(q+i)-t^2a_1a_2)\phi_1(t)\right]. \tag{A.22c}$$

We only need to solve for $\phi_1(t)$ and subsequently use it to find $\phi_2(t)$ and $\phi_3(t)$. The general solution is

$$\begin{aligned}\phi_1(t)=\;&\mathcal{C}_1\frac{t^2}{4}(a_1a_2+a_3a_4)\,{}_1F_2\left[\begin{matrix}1+\frac{ipa_3a_4}{2(a_1a_2+a_3a_4)}\\ 2+\frac{ip}{2}\;\;\frac{3}{2}+\frac{iq}{2}\end{matrix};-\frac{1}{4}t^2(a_1a_2+a_3a_4)\right]+\\&\mathcal{C}_2\left(-\frac{1}{4}\right)^{-\frac{ip}{2}}(-a_1a_2-a_3a_4)^{-\frac{ip}{2}}\,t^{-ip}\,{}_1F_2\left[\begin{matrix}\frac{ipa_3a_4}{2(a_1a_2+a_3a_4)}-\frac{ip}{2}\\ -\frac{1}{2}ip\;\;\frac{i(q-p)}{2}+\frac{1}{2}\end{matrix};-\frac{1}{4}t^2(a_1a_2+a_3a_4)\right]+\\&\mathcal{C}_3\left(-\tfrac{1}{4}\right)^{\frac{(-iq+1)}{2}}(-a_1a_2-a_3a_4)^{\frac{(-iq+1)}{2}}\,t^{-iq+1}\,{}_1F_2\left[\begin{matrix}\frac{ipa_3a_4}{2(a_1a_2+a_3a_4)}-\frac{iq}{2}+\frac{1}{2}\\ \frac{1}{2}-\frac{iq}{2},\;\frac{i(p-q)}{2}+\frac{3}{2}\end{matrix};-\frac{1}{4}t^2(a_1a_2+a_3a_4)\right],\end{aligned} \tag{A.23}$$

where $\mathcal{C}_{1,2,3}$ are arbitrary complex constants that determine the boundary condition.

A.5 Some special solutions of the 3 × 3 model

Consider the following set of differential equations

$$i\begin{pmatrix}\dot{\phi}_1(t)\\ \dot{\phi}_2(t)\\ \dot{\phi}_3(t)\end{pmatrix}=\begin{pmatrix}\frac{\alpha\Delta}{3}-\frac{3}{2\nu t} & \sqrt{\frac{2}{3}}\Delta & -\frac{1}{3}\sqrt{2}\alpha\Delta\\ \sqrt{\frac{2}{3}}\Delta & \frac{2\alpha\Delta}{3} & -\frac{\Delta}{\sqrt{3}}\\ -\frac{1}{3}\sqrt{2}\alpha\Delta & -\frac{\Delta}{\sqrt{3}} & 0\end{pmatrix}\begin{pmatrix}\phi_1(t)\\ \phi_2(t)\\ \phi_3(t)\end{pmatrix}. \tag{A.24}$$

This model is obtained from (A.11) but without the simplification (A.13). Specifically, to obtain (A.24) up to a term proportional to identity, we start with (A.11), perform the transformation (A.12), and set $j_1=j_2=j_3=1/2$ with

$$\epsilon_3=\Delta+\epsilon_1,\quad \epsilon_2=\frac{1}{2}[(1+\alpha)\epsilon_1+(1-\alpha)\epsilon_3]. \tag{A.25}$$

Note that ϵ_1, ϵ_2, and ϵ_3 are the eigenvalues of the Hamiltonian at $t\to\infty$, see (A.11).

Now consider the case $\alpha=\pm1$, which corresponds to $\epsilon_2=\epsilon_1$ or $\epsilon_2=\epsilon_3$, i.e., the eigenvalues at $t\to\infty$ are degenerate. Let $\tau=t\Delta$. At those specific values of α, it turns out that $\phi_2(t)$ and $\phi_3(t)$ are related as

$$A\exp\left(i\frac{\alpha}{3}\Delta t\right)-\alpha\sqrt{3}\phi_3(t)=\phi_2(t). \tag{A.26}$$

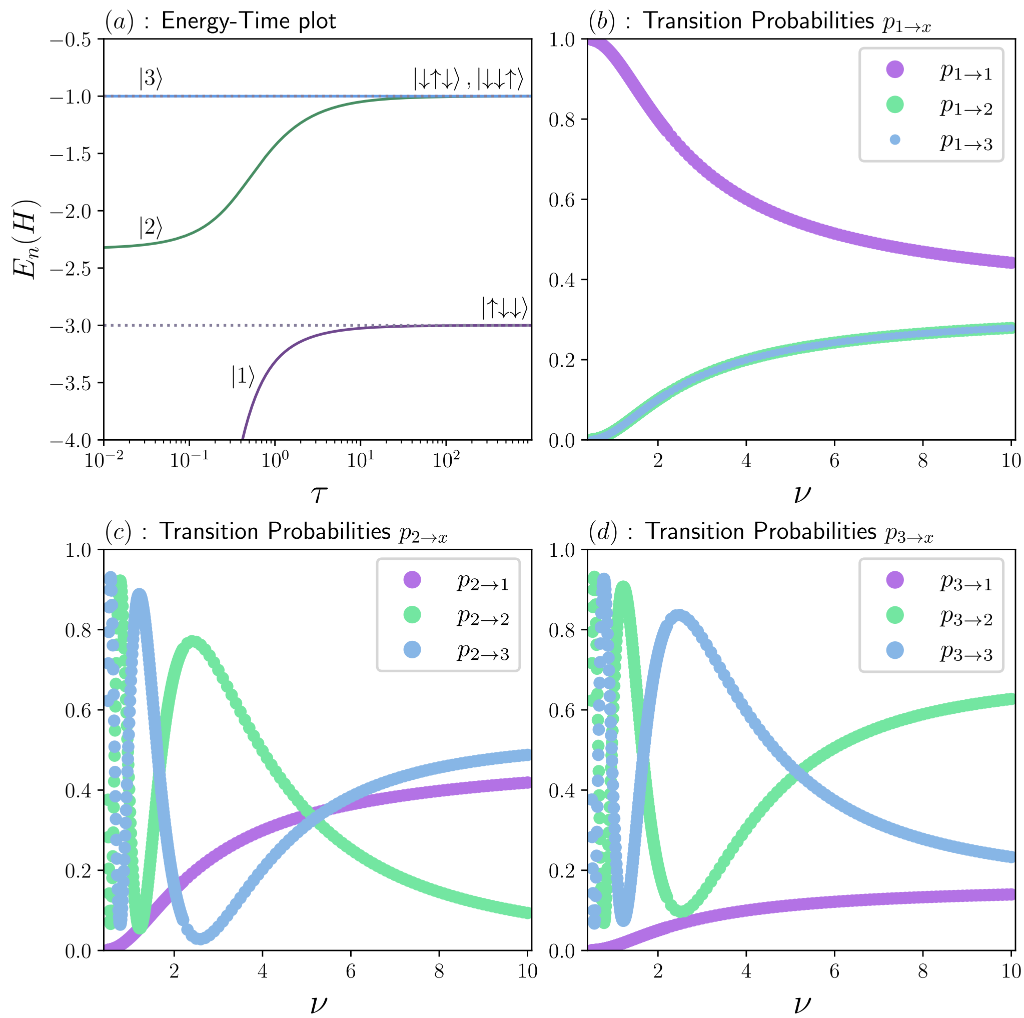

Figure 8: (a) Instantaneous (adiabatic) eigenvalues of the 3×3 HLZ model (55) with $\alpha=-1$, $\epsilon_1=1$, and $\nu=2$ with time $\tau=\Delta t$. The ground state $|1\rangle$ evolves towards $|\uparrow\downarrow\downarrow\rangle$ which represents the lowest energy curve. (b – d) All elements of the transition probability matrices. The scatter plots represent the numerical simulation of $p_{x\to y}$ for different values of ν at time $\tau=10^3$.

This allows us to write the differential equations as

$$-9\sqrt{3}Ae^{\frac{1}{3}i\alpha\tau}+18\nu\tau\ddot{\phi}_3(\tau)+3i\dot{\phi}_3(\tau)(8\alpha\nu\tau-9)+\phi_3(t)(10\nu\tau+27\alpha)=0,$$
$$\left[-\sqrt{\frac{3}{2}\frac{A}{\alpha}}e^{\frac{1}{3}i\alpha\Delta t}-\frac{3i\dot{\phi}_3(t)}{\sqrt{2}\alpha\Delta}+\frac{3\phi_3(t)}{\sqrt{2}}\right]=\phi_1(t), \tag{A.27}$$

whose solutions are given in terms of the Tricomi hypergeometric function U and Generalised Laguerre polynomial L,

$$\phi_3(\tau)=e^{-\frac{1}{3}i(2\alpha+3)\tau}\tau^{1+\frac{3i}{2\nu}}\left[c_1U\left(1+\frac{i(\alpha+3)}{4\nu},2+\frac{3i}{2\nu},2i\tau\right)+c_2L^{1+\frac{3i}{2\nu}}_{-1-\frac{i(\alpha+3)}{4\nu}}(2i\tau)+A\,I(\nu,\tau)\right], \tag{A.28}$$

where

$$I(\nu,\tau)=\int_1^\tau\frac{\sqrt{3}Ae^{i(\alpha+1)x}x^{-2-\frac{3i}{2\nu}}\left(U\left(\frac{i(\alpha+3)}{4\nu}+1,2+\frac{3i}{2\nu},2i\tau\right)L^{1+\frac{3i}{2\nu}}_{-\frac{i(\alpha+3)}{4\nu}-1}(2ix)-U\left(\frac{i(\alpha+3)}{4\nu}+1,2+\frac{3i}{2\nu},2ix\right)L^{1+\frac{3i}{2\nu}}_{-\frac{i(\alpha+3)}{4\nu}-1}(2i\tau)\right)}{4i\nu U\left(\frac{i(\alpha+3)}{4\nu}+1,2+\frac{3i}{2\nu},2ix\right)L^{2+\frac{3i}{2\nu}}_{-\frac{i(\alpha+3)}{4\nu}-2}(2ix)+(\alpha-4i\nu+3)U\left(\frac{i(\alpha+3)}{4\nu}+2,3+\frac{3i}{2\nu},2ix\right)L^{1+\frac{3i}{2\nu}}_{-\frac{i(\alpha+3)}{4\nu}-1}(2ix)}dx. \tag{A.29}$$

We study this analytical solution with the numerical simulations in Fig. 8. It is interesting to note that for $\nu \to 0$, the transition probabilities $p_{i\to j}$ where $i,j \in \{2,3\}$ oscillate heavily as functions of ν.

B Contour integral solution to the KZ equation for 1×1 LZ-Hamiltonians

In this section we detail the contour integral solution to the Hamiltonians in equation (32). The Hamiltonians in question are

$$\begin{aligned} H_{1/2}^{(-1)}(\nu) &= -(\epsilon_1 + \epsilon_2), \\ H_{1/2}^{(1)}(\nu) &= (\epsilon_1 + \epsilon_2) - \frac{1}{\nu t}. \end{aligned} \tag{B.1}$$

Our first observation is that the Hamiltonians in (B.1) are proportional to the single site, spin-$1/2$ ($n = 1,\ s = 1/2$) BCS Hamiltonian:

$$H_{N=1,1/2} = 2\xi \hat{s}^z - \frac{1}{2\nu t}\hat{s}^+\hat{s}^- = 2\xi \hat{s}^z - \frac{1}{2\nu t}(1 + 2\hat{s}^z). \tag{B.2}$$

Specifically, (B.1) are simply equal to $2H_{n=1,1/2}$ where we identify $\xi = (\epsilon_1 + \epsilon_2)/2$. First, let us focus on the Hamiltonian $H_{1/2}^{(-1)}(\nu)$ in (B.1) which corresponds to $s^z = -1/2$ in (B.2). The Yang-Yang action (37) for (B.2) becomes

$$\mathcal{S}(\vec{\lambda}, \xi) = -\nu t \xi. \tag{B.3}$$

The state $|\Phi(\vec{\lambda}, \xi)\rangle$ is simply $|\downarrow\rangle$. Since $M = 0$, there is no integration to be done in equation (36) (the set of λ_α is empty), and we immediately write down the solution,

$$\Psi(t, \vec{\epsilon}) = \oint d\vec{\lambda} e^{-\frac{i}{\nu}S(\vec{\lambda},\xi)} = e^{\left\{\frac{i}{\nu}(\nu t \xi)\right\}} |\downarrow\rangle. \tag{B.4}$$

This result is the same as the solution found by directly solving the non-stationary Schrödinger equation for the Hamiltonian $H_{1/2}^{(-1)}(\nu)$ in (B.1).

The Hamiltonian $H_{1/2}^{(1)}(\nu)$ in (B.1) is slightly less trivial. By directly solving the non-stationary Schrödinger equation, we find (up to normalization)

$$\Psi(t, \xi) = e^{\left\{-\frac{i}{\nu}\left[\xi \nu t - \frac{1}{2}\log(t)\right]\right\}} |\uparrow\rangle. \tag{B.5}$$

For this problem, the off-shell Bethe state as defined in (38) is given by

$$|\Phi\rangle = \prod_\alpha \hat{L}^+(\lambda_\alpha)|\downarrow\rangle = \frac{1}{(\lambda_1 - \xi)}|\uparrow\rangle. \tag{B.6}$$

The Yang-Yang action reads

$$\mathcal{S}(\vec{\lambda}, \xi) = -2\nu t \xi(\frac{1}{2} - 1) + 2\nu t(\lambda_1 - \xi) + \frac{1}{2}\log(\xi - \lambda_1). \tag{B.7}$$

Note that we explicitly added and removed a factor of $2\nu t \xi$ in the first and second term of the action respectively. For a general one-site spin-s BCS Hamiltonian one can always make a simple replacement like this. The solution is then given by

$$\Psi(t, \xi) = \oint d\vec{\lambda} e^{-\frac{i}{\nu}\left[\nu t \xi + 2\nu t(\lambda_1 - \xi) + \frac{1}{2}\log(\xi - \lambda_1)\right]} \frac{1}{(\lambda_1 - \xi)}|\uparrow\rangle. \tag{B.8}$$

Redefining $\lambda_1 - \xi \to \lambda_1$ we find

$$\Psi(t,\xi) = e^{-i\nu t\xi} \oint d\vec{\lambda} e^{-\frac{i}{\nu}\left[+2\nu t\lambda_1 + \frac{1}{2}\log(-\lambda_1)\right]} \frac{1}{\lambda_1} |\Uparrow\rangle = e^{-i\nu t\xi} I(t). \tag{B.9}$$

By comparing Eqs. (B.5) and (B.9), we see that the integral $I(t)$ must equal $e^{\frac{i}{2\nu}\log(t)}$. This can be shown straightforwardly by taking the derivative of $I(t)$. Using the fact that

$$d\lambda_1 \frac{d}{dt}\left(e^{-2it\lambda_1}\right) = \frac{\lambda_1}{t} d\left(e^{-2it\lambda_1}\right), \tag{B.10}$$

we can write (removing an overall constant)

$$\frac{dI(t)}{dt} = \frac{1}{t}\oint d\left(e^{-2it\lambda_1}\right)\lambda_1^{\frac{-i}{2\nu}}. \tag{B.11}$$

Integrating by parts, we find

$$\frac{dI(t)}{dt} = \frac{1}{t}\oint d\left(e^{-2it\lambda_1}\lambda_1^{\frac{-i}{2\nu}}\right) + \frac{i}{2\nu t}\oint d\left(e^{-2it\lambda_1}\right)\lambda_1^{\frac{-i}{2\nu}-1} d\lambda_1. \tag{B.12}$$

Since the boundary term vanishes for a closed contour, we have

$$\frac{dI(t)}{dt} = \frac{i}{2\nu t} I(t) \implies I(t) \propto e^{\frac{i}{\nu}\log(t)}. \tag{B.13}$$

We end this section by noting that the calculation presented in this appendix can be generalized to a arbitrary single-site spin-s BCS Hamiltonian. The calculation will be slightly more difficult, but the procedure remains the same. Let us go through the calculation below.

For a single-site spin-s BCS Hamiltonian of the form (B.2), we find for the Yang-Yang action:

$$S(\vec{\lambda},\xi) = 2\nu t\xi(-s+M) + 2\nu t\sum_{\alpha}^{M}\left[(\lambda_\alpha - \xi) + s\log(\xi - \lambda_\alpha) - \frac{1}{2}\sum_{\beta\neq\alpha}^{M}\log(\lambda_\beta - \lambda_\alpha)\right]. \tag{B.14}$$

Note that we rewrote the first two terms using $s_z = -s + M$. The off-shell Bethe state is

$$|\Phi\rangle = \prod_{\alpha}\hat{L}^{+}(\lambda_\alpha)|\Downarrow\rangle = \left(\prod_{\alpha}^{M}\frac{1}{\lambda_\alpha - \xi}\right)|\Uparrow\rangle. \tag{B.15}$$

The same shift as before, $\lambda_\alpha - \xi \to \lambda_\alpha$, simplifies the final result to

$$\Psi(t,\xi) = e^{-2its_z} F(t)|\Uparrow\rangle, \tag{B.16}$$

where

$$F(t) = \oint d\vec{\lambda} e^{-2it\sum_{\alpha}^{M}\left[\lambda_\alpha + s\log(-\lambda_\alpha) - \frac{1}{2}\sum_{\beta\neq\alpha}\log(\lambda_\beta - \lambda_\alpha)\right]}\prod_{\alpha}\lambda_\alpha^{-1} \tag{B.17}$$

We now do the same as before: differentiate $F(t)$ and use (B.10). The steps remain largely the same, only now we have to sum over $\alpha = \{1,\ldots,M\}$ and keep track of an additional logarithmic term. We find

$$\frac{dF}{dt} = \frac{1}{t}\sum_{\alpha}^{M}\oint\prod_{\beta\neq\alpha}\left(d\lambda_\beta\lambda_\beta^{-1-\frac{is}{\nu}}e^{-2it\lambda_\beta}\right)d\left(e^{-2it\lambda_\alpha}\right)\lambda_\alpha^{-\frac{is}{\nu}}e^{\frac{i}{2\nu}\sum_{\alpha',\beta\neq\alpha'}\log(\lambda_\beta - \lambda_{\alpha'})} \tag{B.18}$$

We integrate by parts as before,

$$\frac{dF}{dt} = -\frac{1}{B}\sum_\alpha^M \oint \prod_\beta \left(d\lambda_\beta \lambda_\beta^{-1-\frac{is}{\nu}} e^{-2it\lambda_\beta + \frac{i}{2\nu}\sum_{\beta'\neq\beta}\log(\lambda_\beta - \lambda_{\beta'})} \right) \left[-\frac{is}{\nu} + \frac{i}{\nu}\sum_{\beta\neq\alpha} \frac{\lambda_\alpha}{\lambda_\beta - \lambda_\alpha} \right]. \tag{B.19}$$

The summation over α simplifies the second term in the square brackets,

$$\sum_\alpha \left[-\frac{is}{\nu} + \frac{i}{\nu}\sum_{\beta\neq\alpha} \frac{\lambda_\alpha}{\lambda_\beta - \lambda_\alpha} \right] = -\frac{i}{\nu}\left[sM - \frac{M(M-1)}{2} \right]. \tag{B.20}$$

We conclude that

$$\frac{dF(t)}{dt} = \frac{i}{t}\left[sM - \frac{M(M-1)}{2} \right] F(t) \implies \Psi(t,\xi) = \mathcal{N} e^{-2its_z + \frac{i}{\nu}\left[sM - \frac{M(M-1)}{2} \right]\log(t)} \left|\uparrow\right\rangle, \tag{B.21}$$

where $\mathcal{N}$ is a normalization constant. This is the same result as the one we obtain through direct integration of (B.2).[6]

References

[1] L. D. Landau, *A theory of energy transfer. II*, Phys. Z. Sowjetunion **2** (1932), doi:10.1016/B978-0-08-010586-4.50014-6.

[2] C. Zener and R. H. Fowler, *Non-adiabatic crossing of energy levels*, Proceedings of the Royal Society of London. Series A, Containing Papers of a Mathematical and Physical Character **137**(833), 696 (1997), doi:10.1098/rspa.1932.0165, Publisher: Royal Society.

[3] E. Majorana, *Atomi orientati in campo magnetico variabile*, Il Nuovo Cimento (1924-1942) **9**(2), 43 (1932), doi:10.1007/BF02960953.

[4] E. C. G. Stueckelberg, *Theory of Inelastic Collisions Between Atoms*, vol. 5, Helvetica Physica Acta, Switzerland (1932).

[5] L. Cifarelli, ed., *Scientific Papers of Ettore Majorana: A New Expanded Edition*, Springer International Publishing, Cham, ISBN 978-3-030-23508-6 978-3-030-23509-3, doi:10.1007/978-3-030-23509-3 (2020).

[6] F. D. Giacomo and E. E. Nikitin, *The Majorana formula and the Landau–Zener–Stückelbergtreatment of the avoided crossing problem*, Physics-Uspekhi **48**(5), 515 (2005), doi:10.1070/PU2005v048n05ABEH002804, Publisher: IOP Publishing.

[7] Y. N. Demkov and V. I. Osherov, *Stationary and nonstationary problems in quantum mechanics that can be solved by means of contour integration*, Soviet Journal of Experimental and Theoretical Physics **26**(5), 916 (1968).

[8] V. N. Ostrovsky and H. Nakamura, *Exact analytical solution of the N-level Landau - Zener-type bow-tie model*, Journal of Physics A: Mathematical and General **30**(19), 6939 (1997), doi:10.1088/0305-4470/30/19/028.

[9] Y. N. Demkov and V. N. Ostrovsky, *Multipath interference in a multistate Landau-Zener-type model*, Physical Review A **61**(3), 032705 (2000), doi:10.1103/PhysRevA.61.032705, Publisher: American Physical Society.

[6] This can be seen straightforwardly by replacing the operators $\hat{s}^+\hat{s}^-$ with $s(s+1) - \hat{s}_z^2 + \hat{s}_z$, resulting in a wavefunction of the form of (B.5) with a prefactor in front of the logaritm equal to the one found in (B.20)

[10] Y. N. Demkov and V. N. Ostrovsky, *The exact solution of the multistate Landau-Zener type model: the generalized bow-tie model*, Journal of Physics B: Atomic, Molecular and Optical Physics **34**(12), 2419 (2001), doi:10.1088/0953-4075/34/12/309.

[11] N. A. Sinitsyn and F. Li, *Solvable multistate model of Landau-Zener transitions in cavity QED*, Physical Review A **93**(6), 063859 (2016), doi:10.1103/PhysRevA.93.063859, Publisher: American Physical Society.

[12] N. A. Sinitsyn, E. A. Yuzbashyan, V. Y. Chernyak, A. Patra and C. Sun, *Integrable Time-Dependent Quantum Hamiltonians*, Physical Review Letters **120**(19), 190402 (2018), doi:10.1103/PhysRevLett.120.190402, Publisher: American Physical Society.

[13] E. A. Yuzbashyan, *Integrable time-dependent Hamiltonians, solvable Landau–Zener models and Gaudin magnets*, Annals of Physics **392**, 323 (2018), doi:10.1016/j.aop.2018.01.017.

[14] A. Patra and E. A. Yuzbashyan, *Quantum integrability in the multistate Landau–Zener problem*, Journal of Physics A: Mathematical and Theoretical **48**(24), 245303 (2015), doi:10.1088/1751-8113/48/24/245303, Publisher: IOP Publishing.

[15] E. A. Yuzbashyan and B. S. Shastry, *Quantum Integrability in Systems with Finite Number of Levels*, Journal of Statistical Physics **150**(4), 704 (2013), doi:10.1007/s10955-013-0689-9.

[16] V. I. Arnold, *Mathematical Methods of Classical Mechanics*, vol. 60 of *Graduate Texts in Mathematics*, Springer, New York, NY, ISBN 978-1-4419-3087-3 978-1-4757-2063-1, doi:10.1007/978-1-4757-2063-1 (1989).

[17] M. Błaszak, K. Marciniak and Z. Domański, *Systematic construction of nonautonomous Hamiltonian equations of Painlevé type. I. Frobenius integrability*, Studies in Applied Mathematics **148**(3), 1208 (2022), doi:10.1111/sapm.12473, _eprint: https://onlinelibrary.wiley.com/doi/pdf/10.1111/sapm.12473.

[18] V. G. Knizhnik and A. B. Zamolodchikov, *Current algebra and Wess-Zumino model in two dimensions*, Nuclear Physics B **247**(1), 83 (1984), doi:10.1016/0550-3213(84)90374-2.

[19] M. Gaudin, *The Bethe Wavefunction*, Cambridge University Press, Cambridge, ISBN 978-1-107-04585-9, doi:10.1017/CBO9781107053885 (2014).

[20] G. Ortiz, R. Somma, J. Dukelsky and S. Rombouts, *Exactly-solvable models derived from a generalized Gaudin algebra*, Nuclear Physics B **707**(3), 421 (2005), doi:10.1016/j.nuclphysb.2004.11.008.

[21] K. Hikami, *Gaudin magnet with boundary and generalized Knizhnik-Zamolodchikov equation*, Journal of Physics A: Mathematical and General **28**(17), 4997 (1995), doi:10.1088/0305-4470/28/17/028.

[22] H. M. Babujian and A. V. Kitaev, *Generalized Knizhnik–Zamolodchikov equations and isomonodromy quantization of the equations integrable via the Inverse Scattering Transform: Maxwell–Bloch system with pumping*, Journal of Mathematical Physics **39**(5), 2499 (1998), doi:10.1063/1.532404.

[23] V. Kurak and A. Lima-Santos, *The A(2)2 Gaudin model and its associated Knizhnik–Zamolodchikov equation*, Journal of Physics A: Mathematical and General **38**(2), 333 (2004), doi:10.1088/0305-4470/38/2/004.

[24] A. Lima-Santos and W. Utiel, *Gaudin magnet with impurity and its generalized knizhnik–zamolodchikov equation*, International Journal of Modern Physics B **20**(15), 2175 (2006), doi:10.1142/S0217979206034595, Publisher: World Scientific Publishing Co.

[25] D. Fioretto, J.-S. Caux and V. Gritsev, *Exact out-of-equilibrium central spin dynamics from integrability*, New Journal of Physics **16**(4), 043024 (2014), doi:10.1088/1367-2630/16/4/043024, Publisher: IOP Publishing.

[26] H. M. Babujian, *Off-shell Bethe ansatz equations and N-point correlators in the SU(2) WZNW theory*, Journal of Physics A: Mathematical and General **26**(23), 6981 (1993), doi:10.1088/0305-4470/26/23/037.

[27] N. Nekrasov, A. Rosly and S. Shatashvili, *Darboux coordinates, Yang-Yang functional, and gauge theory*, Nuclear Physics B - Proceedings Supplements **216**(1), 69 (2011), doi:10.1016/j.nuclphysbps.2011.04.150.

[28] C. N. Yang and C. P. Yang, *One-dimensional chain of anisotropic spin-spin interactions*, Physics Letters **20**(1), 9 (1966), doi:10.1016/0031-9163(66)91024-9.

[29] C. N. Yang and C. P. Yang, *Thermodynamics of a One-Dimensional System of Bosons with Repulsive Delta-Function Interaction*, Journal of Mathematical Physics **10**(7), 1115 (1969), doi:10.1063/1.1664947.

[30] T. H. Koornwinder and J. V. Stokman, eds., *Encyclopedia of Special Functions: The Askey-Bateman Project: Volume 2: Multivariable Special Functions*, vol. 2, Cambridge University Press, Cambridge, ISBN 978-1-107-00373-6, doi:10.1017/9780511777165 (2020).

[31] K. Aomoto and M. Kita, *Theory of Hypergeometric Functions*, Springer Monographs in Mathematics. Springer Japan, Tokyo, ISBN 978-4-431-53912-4 978-4-431-53938-4, doi:10.1007/978-4-431-53938-4 (2011).

[32] A. Zabalo, A.-K. Wu, J. H. Pixley and E. A. Yuzbashyan, *Nonlocality as the source of purely quantum dynamics of BCS superconductors*, Physical Review B **106**(10), 104513 (2022), doi:10.1103/PhysRevB.106.104513, Publisher: American Physical Society.

[33] A. Bandrauk, *On long-range curve crossings*, Molecular Physics **24**(3), 661 (1972), doi:10.1080/00268977200101771, Publisher: Taylor & Francis _eprint: https://doi.org/10.1080/00268977200101771.

[34] R. S. Tantawi, A. S. Sabbah, J. H. Macek and S. Y. Ovchinnikov, *Two-state model for top-of-barrier processes*, Physical Review A **62**(4), 042710 (2000), doi:10.1103/PhysRevA.62.042710, Publisher: American Physical Society.

[35] V. N. Ostrovsky, *Nonstationary multistate Coulomb and multistate exponential models for nonadiabatic transitions*, Physical Review A **68**(1), 012710 (2003), doi:10.1103/PhysRevA.68.012710, Publisher: American Physical Society.

[36] M. Child, *Curve-crossing and the WKB approximation*, Molecular Physics **20**(1), 171 (1971), doi:10.1080/00268977100100171, Publisher: Taylor & Francis _eprint: https://doi.org/10.1080/00268977100100171.

[37] V. I. Osherov and V. G. Ushakov, *Threshold anomaly in S scattering with Coulomb charge exchange*, Physical Review A **53**(5), 3157 (1996), doi:10.1103/PhysRevA.53.3157, Publisher: American Physical Society.

[38] E. E. Nikitin, *The Theory of Nonadiabatic Transitions: Recent Development with Exponential Models*, In P.-O. Löwdin, ed., *Advances in Quantum Chemistry*, vol. 5, pp. 135–184. Academic Press, doi:10.1016/S0065-3276(08)60338-X (1970).

[39] F. H. Mies, *Effects of Anharmonicity on Vibrational Energy Transfer*, The Journal of Chemical Physics **40**(2), 523 (1964), doi:10.1063/1.1725148.

[40] N. A. Sinitsyn, *Exact results for models of multichannel quantum nonadiabatic transitions*, Physical Review A **90**(6), 062509 (2014), doi:10.1103/PhysRevA.90.062509, Publisher: American Physical Society.

[41] R. Feynman, J. Hollingsworth, M. Vennettilli, T. Budner, R. Zmiewski, D. P. Fahey, T. J. Carroll and M. W. Noel, *Quantum interference in the field ionization of Rydberg atoms*, Physical Review A **92**(4), 043412 (2015), doi:10.1103/PhysRevA.92.043412, Publisher: American Physical Society.

[42] P. W. Anderson, *Random-Phase Approximation in the Theory of Superconductivity*, Physical Review **112**(6), 1900 (1958), doi:10.1103/PhysRev.112.1900, Publisher: American Physical Society.

[43] J. Bardeen, L. N. Cooper and J. R. Schrieffer, *Theory of Superconductivity*, Physical Review **108**(5), 1175 (1957), doi:10.1103/PhysRev.108.1175, Publisher: American Physical Society.

[44] R. W. Richardson, *Pairing in the limit of a large number of particles*, Journal of Mathematical Physics **18**(9), 1802 (1977), doi:10.1063/1.523493.

[45] H. Bateman, *Higher Transcendental Functions [Volumes I-III]*, McGraw-Hill Book Company (1953).

[46] S. Barik, L. Bakker, V. Gritsev and E. A. Yuzbashyan, *Knizhnik-Zamolodchikov equations and integrable Landau-Zener models - Code*, Zenodo (2024), doi:10.5281/zenodo.11620326.